Accelerating Cleanup of the Defense Nuclear Legacy

Quarterly Technical Progress Report
for the period
July 1, 2008 – August 31, 2008

Dr. W. Glenn Steele, Interim Principal Investigator

Report No. 07040R07

Prepared for the U.S. Department of Energy
Agreement No. DE-FC01-06EW-07040

Institute for Clean Energy Technology
Mississippi State University
205 Research Boulevard
Starkville, MS 39759

icet@icet.msstate.edu
www.icet.msstate.edu

Acknowledgement
This material is based upon work supported by the Department of Energy under award number DE-FC01-06EW-07040

Table of Contents

List of Figures

List of Tables

EXECUTIVE SUMMARY

Task 1. Modeling and Experimental Support for High-Level SRS Salt Disposition Alternatives

Additional calculations on the aqueous phase streams resulting from the dissolution of SRS Tank 25 saltcake using the Defense Waste Processing Facility (DWPF) recycle stream as a diluent are presented. The initial temperature for the saltcake dissolution portion of the simulations was taken as 30^{o}C. This temperature is somewhat higher than that expected (23^{o}C) for processing the waste in the Salt Waste Processing facility (SWPF). Consequently, the simulation started with cooling the individual streams and then deciding on whether to dilute the stream with water, to re-dissolve particles and on the need to add the high hydroxide leachate from Batch 5 sludge processing. For the early dissolution streams, the addition of water dissolved the reprecipitated particles that formed upon cooling. The compositions for both transfer stream 1 and 2 were within corrosion control guidelines and no further processing is anticipated. Solids dissolution for all of the other transfers streams examined (3-8) was accomplished using water only; however, the streams were not within the applicable corrosion standards. The addition of the Batch 5 leachate was however successful in achieving the corrosion conditions. More of the Batch 5 leachate was needed at transfer streams generated at higher levels of initial dilution. The simulations indicate that the Batch 5 leachate stream will be useful as an additive for maintaining the hydroxide and nitrite levels in the waste such that corrosion protection can be maintained.

Results for solids analysis of samples obtained from the Parsons CSSX process testing are also presented. Based upon analytical results, the predominant solids appear to be cancrinite/sodalite mixtures or cancrinite/sodalite/trona mixtures with low weight percentages of gibbsite and iron oxide in all of the dry solids investigated.

Task 2. Process Improvements for the Defense Waste Processing Facility (DWPF)

Laser induced breakdown spectroscopy (LIBS) is a diagnostic technique that can measure the concentrations of various elements in a test sample. This project evaluates LIBS as an on-line, simultaneous multi-species analysis of the slurry sample for Defense Waste Processing Facility. During this work period, efforts on improving the analytical performance of slurry measurement continued. Various experimental configurations and experimental parameters were tested to obtain the optimized experimental condition to direct sampling slurry sample. Calibration data for slurry were recorded by addition of various amount of chemical into the slurry. Slurry analyses were performed with both univariate and multivariate calibration methods.

Task 3. High Efficiency Particulate Air

The Institute for Clean Energy Technology (ICET) at Mississippi State Univeristy (MSU) has been involved in evaluating the performance of AG-1 HEPA filters for several years. A number of 12”x12”x11.5” filters have been loaded with a variety of aerosol challenges that include potassium chloride (KCl), iron salts, and soot. Filter testing has involved different media velocities and particle size distributions of the aerosol challenge

Task 4. Support of Hanford Single Shell Tank Waste Disposition

Development of a neural network to augment the chemistry in HTWOS, specifically for the C tank farm retrieval continued. An ESP program process model using the Modified Sluicing with Recycle (MSwR) and the Mobile Retrieval System (MRS) was used to simulate the retrieval of waste from C-104, C-112, and C-111 into AN-101. C-104 and C-112 retrievals were simulated as MSwR while the retrieval of C-111 was simulated as MRS.

Task 5. Long-Term Monitoring of Selected Heavy Metal and Radionuclide Contaminants and Application of Phytoremediation

During this quarter, we conducted a series of chamber study on foliage uptake of Hg by Indian mustard and two varieties of ferns (Boston fern and Chinese brake fern) under various Hg concentrations. Kinetics of Hg evaporated from contaminated Oak Ridge soils with various Hg sources were examined as well.

Task 6. Saltsone

This project is designed to assist the Savannah River Site (SRS) in the production of the Saltstone waste form from low-level tank waste. The expectation of increased aluminum content in the next batch has raised concerns about an excess heat of hydration, which may create problems for the storage of the waste form. The facility also relies on vault temperature modeling to protect vault temperature limits. These studies are designed to examine the effects of the heat created by the reactions and to discover methods for either dealing with the excess heat or preventing it from occurring in the first place.

Task 7. Bioavailability studies of mercury and other heavy metal contaminants in ecosystems of selected DOE sites

During this quarter, a series of studies on oxidation kinetics of pure HgS and HgS contaminated Oak Ridge soils by two common iron oxides (Fe_2O_3 and Fe_3O_4), which are in the subsurface of Oak Ridge site, were conducted. The results show that oxidation rate of HgS from contaminated

Oak Ridge soil was initially fast and increased until 30 min, then followed by a plateau. The 80-90% of S in the reaction system was SO_4 with a small amount of other intermediate S species.

Task 8. Hanford Tank Inspection

At the end of the previous quarter, ICET was informed that because of the downward revision of the ICET Cooperative Agreement CA08 budget, that there are no funds to support the Hanford in-tank characterization effort for the current Cooperative Agreement year. ICET administrators subsequently issued a stop-work order. The bi-weekly conference calls with our Hanford collaborators were suspended. At this time, no further efforts are planned until funding becomes available.

Task 1

Support of SRS Salt Disposition

Jeffrey S. Lindner and Laura T. Smith

INTRODUCTION

Major needs in the SRS tank farms are dictated by the desire to separate actinides and cesium from salt wastes permitting the processing of the high activity waste fraction in the Defense Waste Processing Facility (DWPF) and stabilization of the lower activity waste as saltstone. Towards this end, efforts are currently underway for the development of the Salt Waste Processing Facility (SWPF) containing the Actinide Removal Process (ARP) and Caustic Side Solvent Extraction Unit (CSSX).[1-3] Current progress involves the pilot-scale testing of the CSSX process wherein solids re-precipitation and emulsions formation has been observed within the contactors and in wash and scrub liquors.

In addition the processing of sludge (caustic addition to Batch 5) to reduce the fraction of aluminum routed to the DWPF is scheduled for FY'08. [4-6]. It is expected that aluminum-rich supernatants will be processed in the same manner as salt waste. Here, however, the downstream implications of mixing the aluminum-rich supernatant with DDA fractions from salt waste retrieval and other streams such as the DWPF recycle are unknown. The silicon concentration within the DWPF recycle stream along with the high aluminum loading in the Batch 5 (and potentially other sludge batches) leachate may indicate the formation of intractable aluminosilicates which will create a downstream problem owing to negligible solubility and the propensity for co-precipitation of uranium.

This project is divided into 2 Tasks. Task 1.1 is aimed at evaluation of the CSSX process through experiments and thermodynamic modeling. In collaboration with Parsons Engineering, the analysis of solids and scales observed in various portions of the process, including contactors, filters and solids formed in drain tanks. These solids will be analyzed using x-ray diffraction and inductively coupled plasma emission spectroscopy. Laboratory kinetic experiments are also planned to examine the stability of simulants to be used in pilot-scale testing at Parsons.

Task 1.2 is aimed at assessing stream stability for blended compositions arising from potential tank farm operations. Any stream blending will be performed upstream of the SWPF. The primary streams of concern are the DWPF Recycle stream, which consists of DWPF overheads and is routed to the tank farm, high aluminum concentration streams from sludge leaching operations (50% NaOH) and dissolved salt streams originating from saltcake dissolution. Predicted compositions will be assessed through calculated parameters such as percent solids by weight, aqueous phase density, adherence to

corrosion waste acceptance criteria, [7] and ionic strength. Initial examination of blending along with the results from Task 1.1 allow for a starting point for SWPF waste acceptance criteria. [8]

WORK ACCOMPLISHMENT

Task 1.1 Previous testing of the CSSX process at two facilities [9] exhibited unexpected solid and emulsion phases inside the contactors, piping, and vessels. ICET personnel were requested to identify several solids samples in addition to the emulsion and organics that may be involved in the solids formation. Seven samples were received from Parsons at ICET for analysis of solids found within an emulsion, an organic/aqueous solution, wet or dry, and are listed in Table 1.

Table 1. Sample identification numbers, date collected, and type.

ID number	Date collected	Type of Sample
HB-X-X-025	8/23/2007	emulsion
P-X-X-655	6/25/2007	Aqueous/solid
P-X-X-644	6/22/2007	Moist solid
P-X-X-643	6/22/2007	Dry solid
P-X-X-645	6/22/2007	Dry solid
P-X-X-639	6/24/2007	Moist solid
T-X-A-027	1/8/2008	Dry solid

The dry solid samples were first analyzed using a Rigaku Ultima III XRay Diffractometer and resulting phases were identified using JADE software. The samples were analyzed as received such that impurities may exist in trace amounts. Best matches from ICDD/ICSD databases are listed by sample number in Table 2.

Table 2. XRD solid results.

Sample	**Primary Phases**
P-X-X-644	$NaNO_3$ Nitratine PDF#97-006-7287 $Na_3(CO_3)(HCO_3)(H_2O)_2$ Trona PDF#97-003-4627 $Na_8(SO_4)(Al_6Si_6O_{24})$ Nosean PDF#97-003-3685
P-X-X-643	$Na_8(AlSiO_4)_6(Cl)_2$ Sodalite

	PDF#97-009-8818 $Na_{97.21}(Si_{96..96}Al_{95.04}O_{384})(H_2O)_{254.64}$ Zeolite PDF#97-008-6644 $Na_3(HCO_3)(CO_3)(H_2O)_2$ Trona PDF#97-003-0655
P-X-X-645	$Na_{7.14}Al_6Si_{7.08}O_{26.73}(H_2O)_{4.87}$ Cancrinite PDF#97-002-8521 $Na_{7.88}(AlSiO_4)_6(CO_3)_{0.93}$ Sodalite PDF#97-041-0144 $Na_3(HCO_3)(CO_3)(H_2O)_2$ Trona PDF#97-003-0655
P-X-X-639	$Na_{7.92}(AlSiO_4)_6(NO_3)_{1.74}(H_2O)_{2.34}$ Cancrinite PDF#97-041-1048 $Na_{7.88}(AlSiO_4)_6(CO_3)_{0.93}$ Sodalite PDF#97-041-0144
T-X-A-027	$Na_{7.66}(Al_6Si_6O_{24})(CO_3)(H_2O)_{3.3}$ Cancrinite PDF#97-041-0523 $Na_8(AlSiO_4)_6(NO_3)_2$ Sodalite PDF#97-041-3035

Sample P-X-X 644 XRD spectra as shown in Figure 1 was significantly different from the others. The sample was analyzed as a moist solid and sodium nitrate appeared upon drying during the data collection. Further analysis of this sample is underway to remove any soluble solids for weight percent calculations.

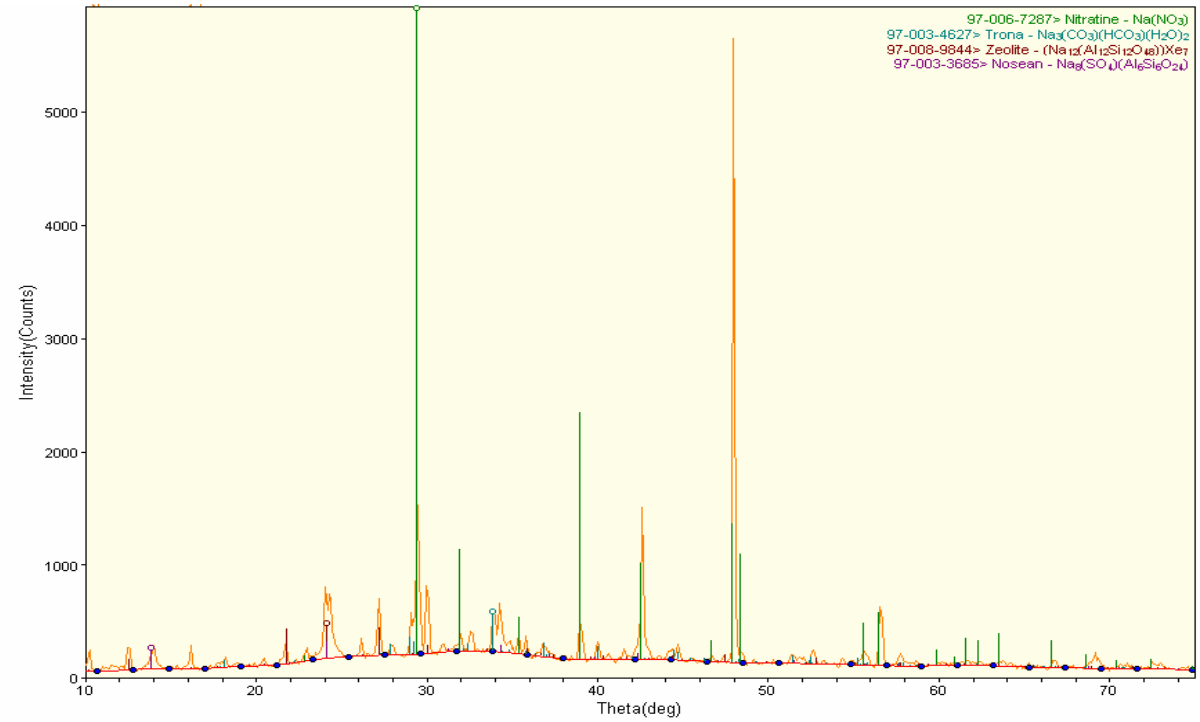

Figure 1. XRD spectra of P-X-X 644 moist solid sample.

Figures 2-5 are the XRD spectra of the remaining solid samples analyzed to date.

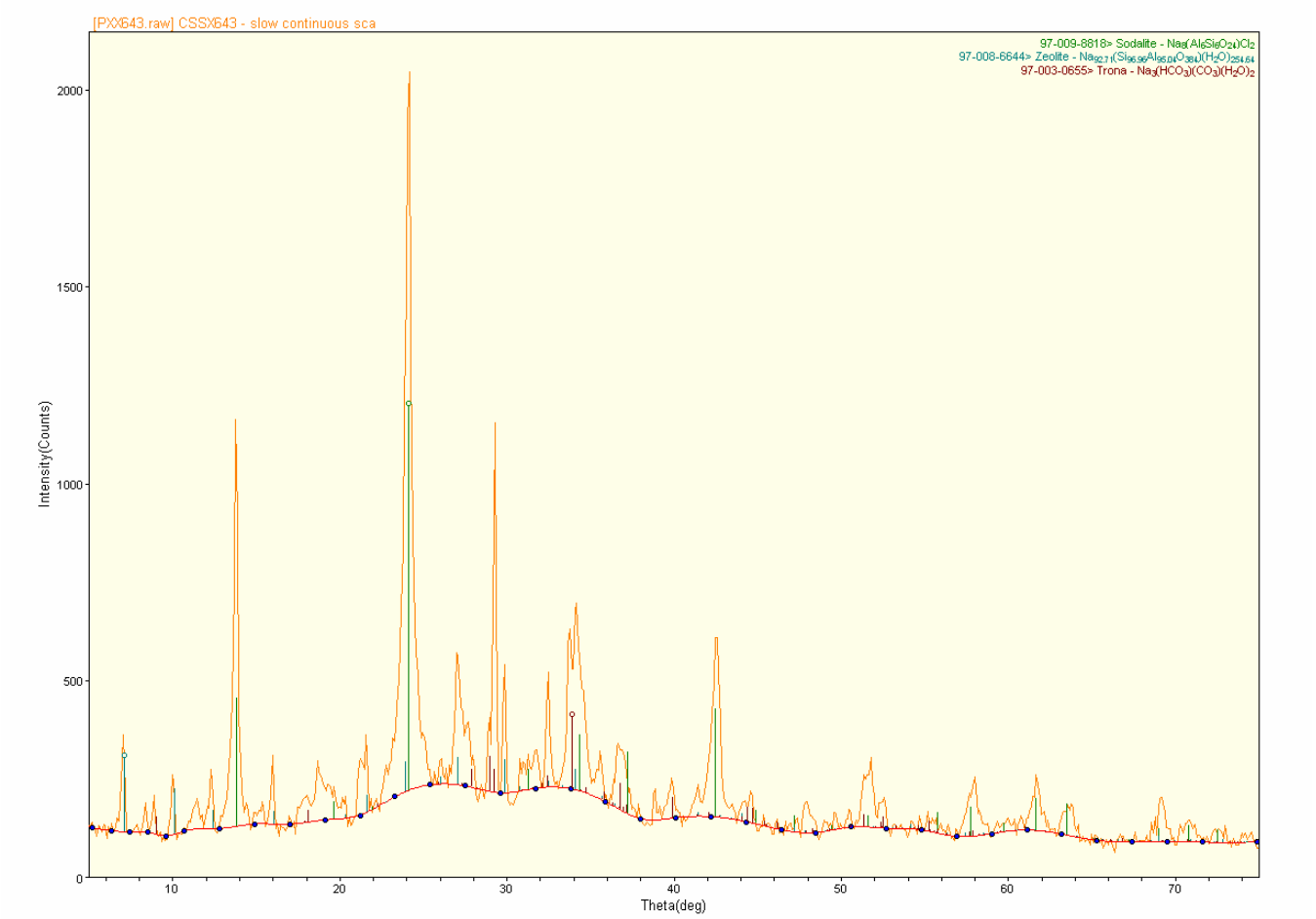

Figure 2. XRD spectra of solid sample P-X-X 643.

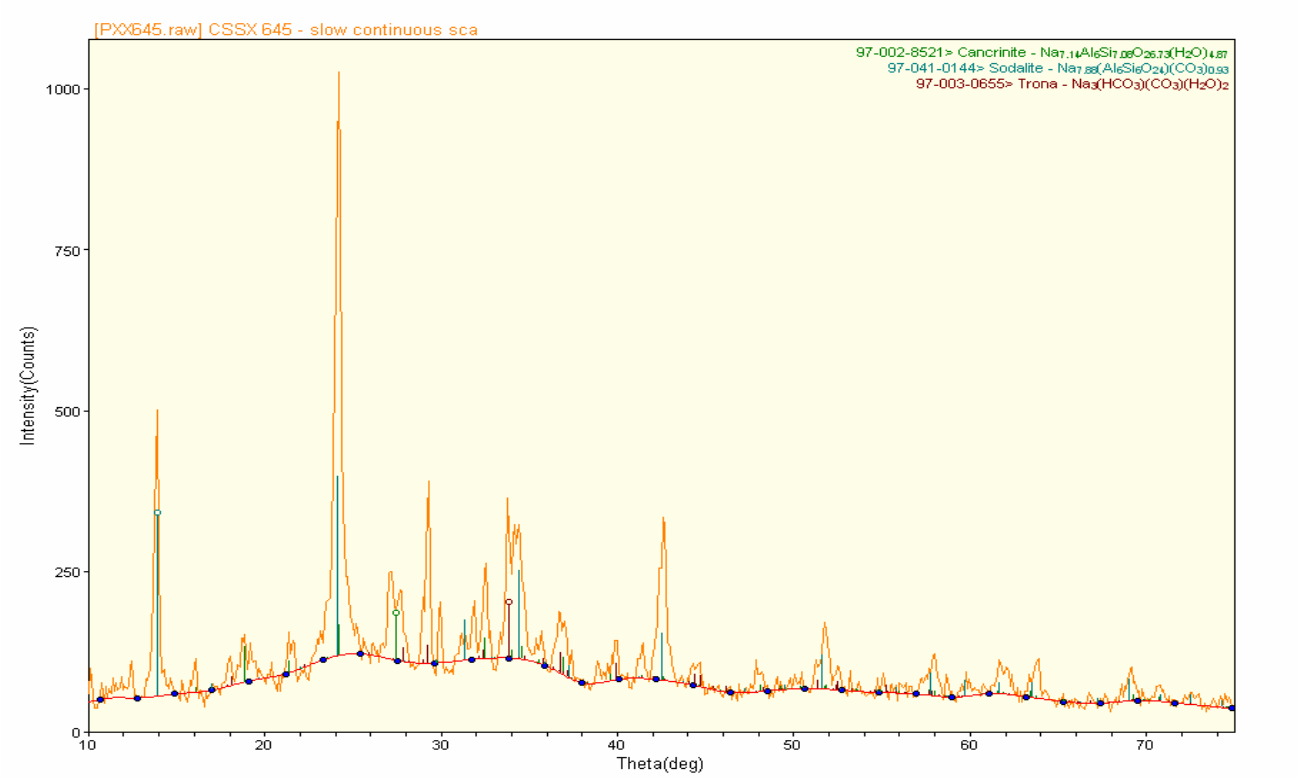

Figure 3. XRD spectra of solid sample P-X-X 645.

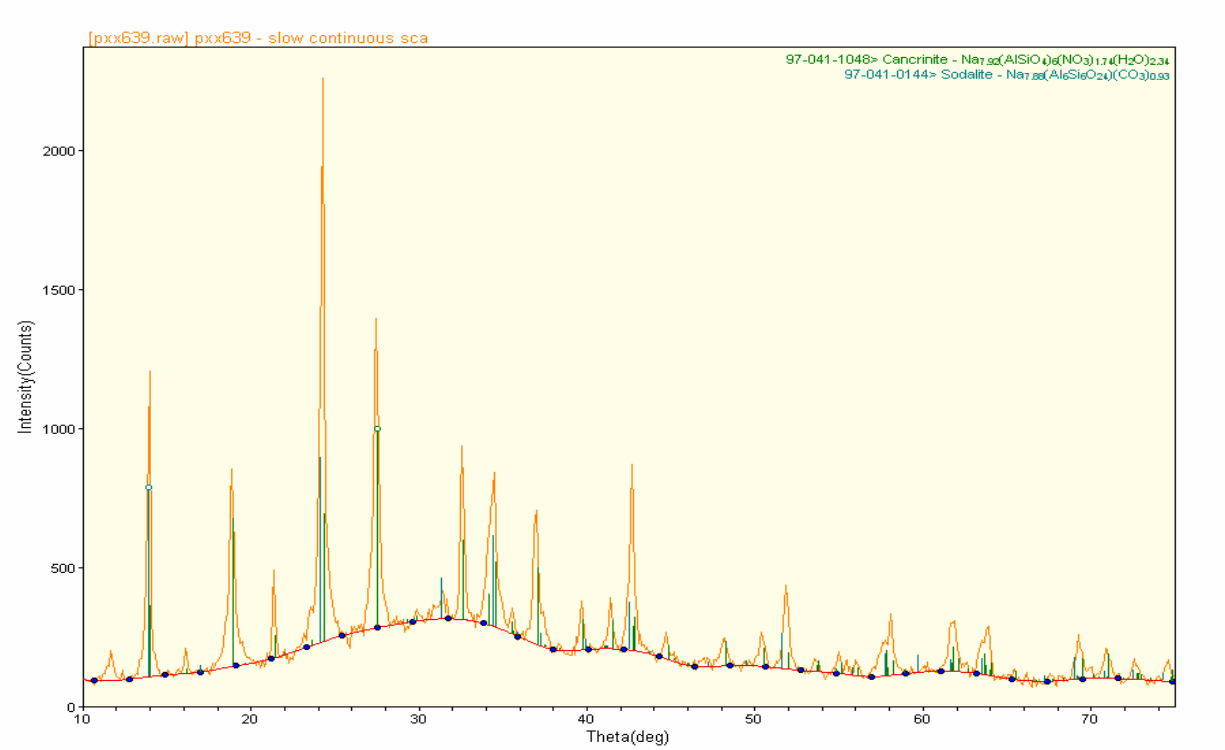

Figure 4. XRD spectra of solid sample P-X-X 639.

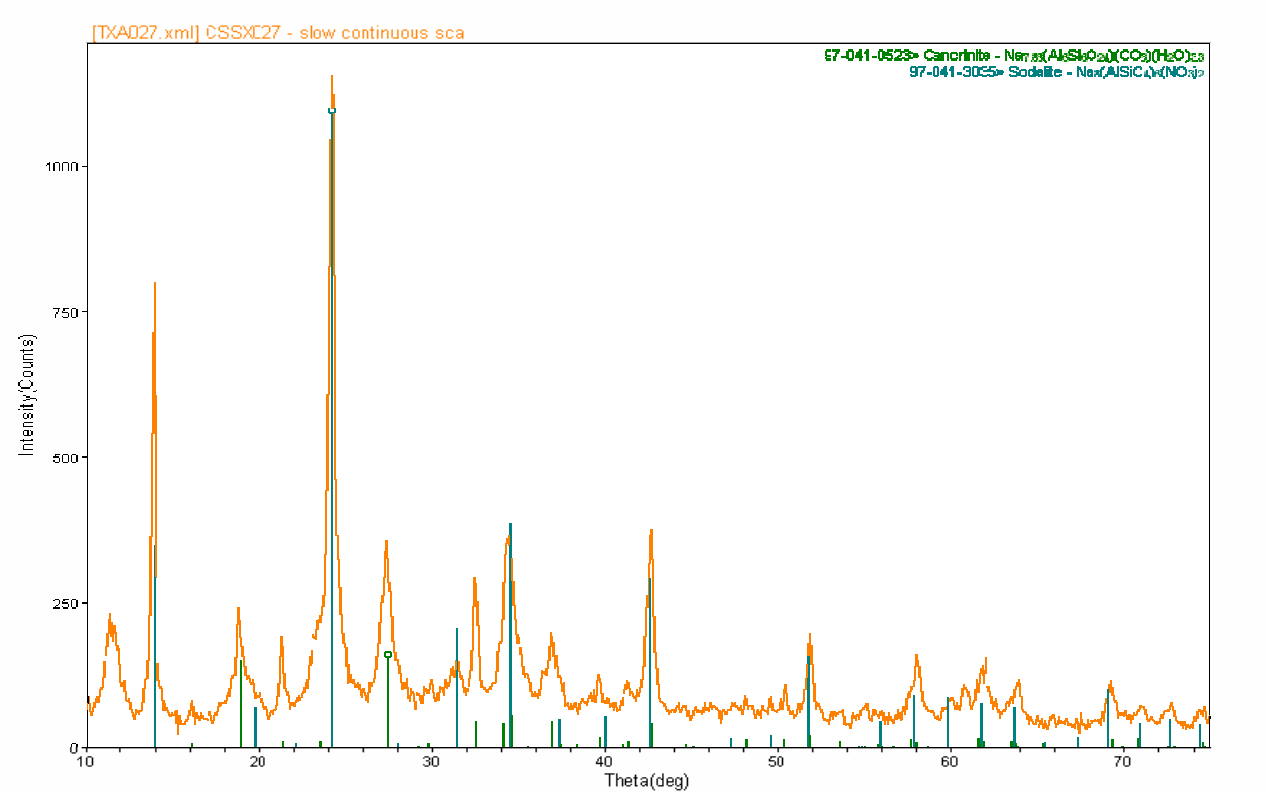

Figure 5. XRD spectra of solid sample T-X-A-027.

ICP analysis was performed on these samples to obtain weight percentages of major components. Table 3 includes weight percentages of aluminum, silicon, sodium, and iron found within the solid samples examined.

Table 3. ICP weight percent results from solid samples.

Analyte (wt %)	PXX639	TXA027	PXX643	PXX645
Al	10.1	14.5	12.3	12.0
Fe	0.05	0.16	0.27	0.14
Na	16.4	13.9	17.2	17.2
Si	9.19	12.9	11.1	10.6

Calculations were performed using the formula weights obtained in XRD results and combined with the ICP weight percentages to determine total calculated components and these results are shown in Table 4. Sodium aluminosilicates (NAS) are the combined cancrinite/sodalite percentages. Formula weights from each component are shown in Table 5.

Table 4. Calculated component weight percentage.

Sample ID	NAS	Fe_2O_3	Gibbsite	Trona	Other Na compounds
PXX639	70.4	0.4	4.8		24.5
TXA027	92.5	0.3	7.2		
PXX643	73.2	0.4	5.4	21.0	
PXX645	66.2	0.2	8.0	25.6	

Table 5. Formula and molecular weights for compounds found in analyses.

Compound	Formula	Formula weight (g/mol)
Cancrinite*(a)*	$Na_{7.92}(AlSiO_4)_6(NO_3)_{1.74}(H_2O)_{2.34}$	1046.5111
Cancrinite*(b)*	$Na_{7.66}(Al_6Si_6O_{24})(CO_3)(H_2O)_{3.3}$	1009.9491
Sodalite*(a)*	$Na_{7.88}(AlSiO_4)_6(CO_3)_{0.93}$	951.3558
Sodalite*(b)*	$Na_8(AlSiO_4)_6(NO_3)_2$	1022.3158
Trona	$Na_3(HCO_3)(CO_3)(H_2O)_2$	226.0262
Gibbsite	$Al(OH)_3$	78.0036
Iron Oxide	Fe_2O_3	159.6922

(a) from sample PXX639
(b) from sample TXA027

Task 1.2

Salt cake Dissolution of Tank 25F Waste using the DWPF Recycle Stream as Diluent – Preparation of the transfer streams for processing in the SWPF.

Previous calculations described the dissolution of the waste in SRS tank 25F using the dilute streams from caustic addition to the DWPF recycle [10]. The composition of the waste contained in Tank 25F, based on core sample analysis conducted at SRNL, was largely $NaNO_3$ [11]. Dilution of the waste with the recycle stream did not result in the prediction of sodium aluminosilicate solids formation. Determination of the volume of the resulting aqueous phase from the tank was made using the initial volume fractions of the waste and assuming a porosity of 30%. Physical properties and chemical concentrations of the dissolution streams are collected in Table 6.

The dissolution calculations were performed at a temperature of 30°C. Current operating parameters for the SWPF are based on a stream temperature of 23°C. Consequently, streams 1-10 of Table 6 were modeled, Figure 6, using heat exchange blocks (30-27-23°C) followed by mix/separate blocks describing the addition of water and the subsequent addition of the Batch 5 leachate solution (23°C). The water was used to dissolve any solids that were precipitated upon lowering the temperature. The major properties of the leachate composition are the low ionic strength (5.37), the moderate pH (14.7) and the high aluminum (~0.77M) and high "free" hydroxide (~3.6M) concentrations.

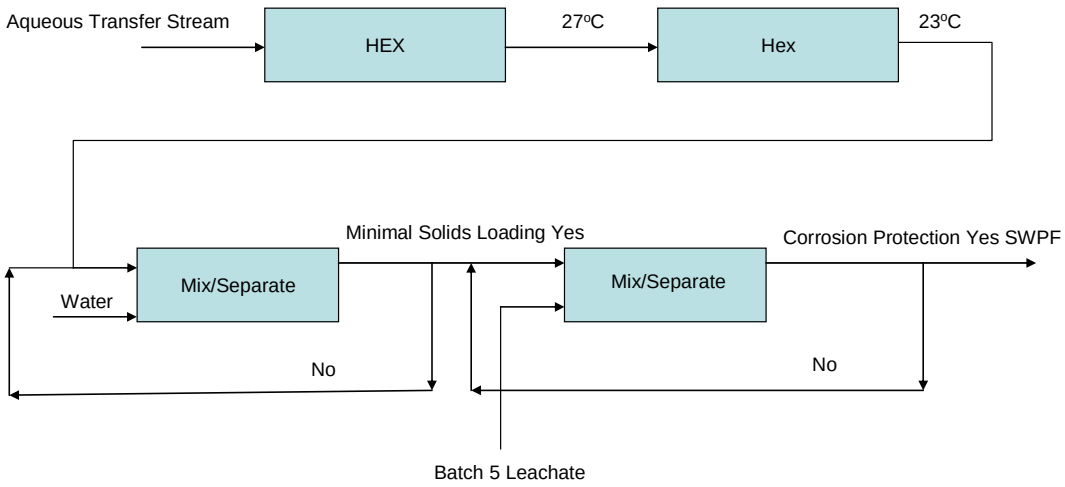

Figure 6. ESP flowsheet for transfer stream processes prior to the SWPF.

The above calculations are somewhat different than those presented previously [10]. In the earlier calculations, the transfer streams were cooled followed by only the addition of the Batch 5 leachate, i.e., no water was used to dissolve reprecipitated solids. The value of the approach detailed here is that less of the Batch 5 leachate stream may be needed and lower solids loadings will initial result based on the solvation power of water as compared to the Batch 5 leachate (density of 1 as opposed to 1.18g/cm^3).

Table 6. Physical properties and ion concentrations (M) of the transfer streams.

Stage	0	1	2	3	4	5	6	7	8	9	10
% dilution by wt	0	11.91	24.65	37.39	50.13	62.86	75.60	88.34	101.08	113.81	126.55
Total (kg)	1.99E+06	2.11E+06	2.20E+06	2.07E+06	2.14E+06	2.14E+06	2.36E+06	1.75E+06	1.05E+06	1.02E+06	1.02E+06
Volume (L)	1.44E+06	1.52E+06	1.58E+06	1.50E+06	1.55E+06	1.54E+06	1.61E+06	1.33E+06	9.75E+05	9.68E+05	9.66E+05
Density (g/L)	1381.62	1384.17	1389.78	1385.08	1383.23	1382.64	1381.82	1312.72	1075.65	1056.58	1050.77
pH	15.12	14.73	14.48	14.19	14.01	13.91	13.88	13.65	13.43	13.44	13.44
Ionic Strength	12.43	12.06	12.17	11.80	11.68	11.64	11.53	8.29	1.98	1.53	1.38
Na^{+}	9.06	8.76	8.77	8.55	8.47	8.44	8.35	6.63	1.71	1.34	1.24
NO_3^{-}	4.19	5.35	5.80	6.37	6.61	6.70	6.93	5.58	0.40	0.08	0.06
OH^{-}	2.99	1.61	0.92	0.57	0.41	0.34	0.32	0.35	0.44	0.45	0.45
Al^{+3}	0.81	0.38	0.22	0.11	0.08	0.06	0.06	0.04	0.04	0.05	0.05
NO_2^{-}	0.65	0.34	0.31	0.30	0.29	0.29	0.29	0.32	0.39	0.40	0.40
CO_3^{-2}	0.18	0.46	0.65	0.41	0.29	0.24	0.18	0.10	0.11	0.11	0.11
SO_4^{-2}	4.71E-02	8.75E-02	1.06E-01	1.81E-01	2.41E-01	2.73E-01	1.81E-01	4.29E-02	2.84E-03	3.71E-04	2.32E-04
F^{-}	1.44E-02	9.68E-03	8.36E-03	6.01E-03	5.28E-03	5.12E-03	8.01E-03	1.82E-02	1.55E-02	9.26E-04	1.05E-04
Si^{+4}	0.00E+00	0.00E+00	1.84E-04	2.82E-04	3.26E-04	3.44E-04	3.48E-04	3.88E-04	4.81E-04	4.88E-04	4.89E-04
$C_2O_4^{-2}$	1.05E-03	2.70E-03	4.14E-03	5.07E-03	5.51E-03	5.70E-03	6.01E-03	9.37E-03	5.13E-02	6.59E-02	2.73E-02
PO_4^{-3}	2.73E-05	3.14E-05	5.21E-05	0.000115	0.000193	0.000251	0.000225	0.000314	0.028603	0.001607	8.39E-05
K^{+}	0.053564	0.028015	0.013425	0.005678	0.002151	0.000672	0.000361	5.14E-05	3.15E-06	1.77E-07	9.54E-09
Cl^{-}	0.011483	0.006006	0.002878	0.001217	0.000461	0.000144	7.73E-05	1.1E-05	6.75E-07	3.8E-08	2.05E-09
U^{+4}	0.00E+00	0.00E+00	4.28E-07	6.55E-07	7.57E-07	7.99E-07	8.09E-07	8.82E-07	1.03E-06	1.06E-06	1.05E-06
Tc^{+4}	0.00E+00	0.00E+00	3.57E-07	5.46E-07	6.31E-07	6.66E-07	6.74E-07	7.51E-07	9.30E-07	9.45E-07	9.47E-07
Cs^{+}	2.96E-07	1.55E-07	1.75E-07	1.85E-07	1.90E-07	1.91E-07	1.92E-07	2.12E-07	2.62E-07	2.67E-07	2.67E-07
Am^{+3}	0.00E+00	0.00E+00	5.21E-08	7.97E-08	9.21E-08	9.73E-08	9.85E-08	1.10E-07	1.36E-07	1.38E-07	1.38E-07
Pu^{+4}	0.00E+00	0.00E+00	6.06E-09	3.06E-09	1.41E-09	9.43E-10	8.20E-10	1.22E-09	1.00E-08	1.18E-08	1.21E-08

Detailed stream physical and chemical properties are given for the processing of transfer stream 4 in Tables 7 and 8. The dilutions correspond to 5% by volume water and then 20% by volume total (5% water and 15% Batch 5 leachate).

Table 7. Aqueous phases and ion concentrations on cooling and dilution of transfer stream 4 first with water, then with the Batch 5 leachate.

	Transfer Stream 4	T4	T4		
Temperature (^{o}C)	30	27	23	23	23
% dilution by Volume	0	0	0	5% water	5% water + 15% leachate
Aqueous					
H_2O (kg)	1.10E+06	1.10E+06	1.10E+06	1.17E+06	1.39E+06
Concentration (M)					
Na^{+}	8.47E+00	8.36E+00	8.23E+00	8.14E+00	7.76E+00
NO_3^{-}	6.61E+00	6.49E+00	6.33E+00	6.36E+00	5.61E+00
OH^{-}	4.07E-01	4.22E-01	4.39E-01	4.13E-01	8.40E-01
NO_2^{-}	2.91E-01	2.94E-01	2.99E-01	2.80E-01	2.92E-01
CO_3^{-2}	2.91E-01	2.95E-01	2.99E-01	2.80E-01	2.49E-01
SO_4^{-2}	2.41E-01	2.43E-01	2.47E-01	2.31E-01	2.05E-01
Al^{+3}	7.50E-02	6.63E-02	5.59E-02	5.05E-02	9.27E-02
$C_2O_4^{-2}$	5.51E-03	5.49E-03	5.41E-03	5.30E-03	4.73E-03
F^{-}	5.28E-03	5.31E-03	5.36E-03	5.03E-03	4.56E-03
Hg^{+2}	1.01E-04	1.02E-04	1.04E-04	9.72E-05	3.80E-03
K^{+}	2.15E-03	2.18E-03	2.21E-03	2.07E-03	2.09E-03
Cl^{-}	4.61E-04	4.66E-04	4.73E-04	4.43E-04	1.04E-03
Si^{+4}	3.26E-04	3.29E-04	3.34E-04	3.13E-04	2.75E-04
Total (kg)	2.14E+06	2.11E+06	2.08E+06	2.21E+06	2.48E+06
Volume (L)	1.55E+06	1.53E+06	1.51E+06	1.61E+06	1.83E+06
Density (g/L)	1383.23	1381.30	1378.51	1375.67	1355.09
pH	14.01	14.10	14.23	14.18	14.43
Ionic Strength	11.68	11.43	11.09	10.94	10.02

Addition of the water served to dissolve the sodium nitrate that reprecipitated upon cooling of the stream from 30 to 23^{o}C, Table-8. After the addition, the model predicted the sum of [OH] + [NO_2] to be ~0.7M. This value is considerably less than that required, 1.1M [7]. Other solids, such as sodium oxalate ($Na_2C_2O_4$) and natrophosphate ($Na_7F(PO_4)_2.19H_2O$) were predicted to reprecipitate upon cooling however, after the addition of water the total solids loading remained small at 0.12% by weight, Table 8.

Simulations were initially performed using only the water dilution portion of the flowsheet, Figure 6. Typically, dilutions were carried out to evaluate the sum of the hydroxide and nitrite concentrations, for predicting corrosion protection, and the percent solids by weight, which amount to a potential perturbation on the CSSX process, Figure 7.

Table 8 Additional physical parameters associated with processing of transfer stream 4. All solids loadings are in kg.

	Transfer Stream 4	T4	T4		
Temperature (^{o}C)	30	27	23	23	23
% dilution by Volume	0	0	0	5% water	5% water + 15% leachate
Solids					
$Al(OH)_3$		1.15E+03	2.48E+03	2.71E+03	6.87E+03
$Na_2C_2O_4$	1.27E-02	1.80E+01	4.92E+01		6.05E+01
Fe_2O_3		2.42E-03	5.10E-03	5.32E-03	1.23E-02
$Na_7F(PO_4)_2.19H_2O$		3.78E+01	6.72E+01	5.77E+01	1.32E+02
$Ca_5(PO_4)_3F$		1.05E-02	2.19E-02	1.46E-02	9.93E-02
$Mg(OH)_2$					3.78E-05
$NaNO_3$		2.61E+04	5.88E+04		
Total (kg)	1.27E-02	2.73E+04	6.14E+04	2.77E+03	7.06E+03
Volume (L)	5.45E-03	1.21E+04	2.71E+04	1.14E+03	2.91E+03
Density (g/L)	2339.99	2263.26	2263.16	2421.53	2422.60
Total Stream					
Total (kg)	2.14E+06	2.14E+06	2.14E+06	2.22E+06	2.49E+06
Volume (L)	1.55E+06	1.54E+06	1.53E+06	1.61E+06	1.84E+06
Density (g/L)	1383.23	1388.21	1394.16	1376.41	1356.78
% solids by wt	0.00	1.28	2.87	0.12	0.28
% water by wt	51.29	51.29	51.29	52.99	55.64

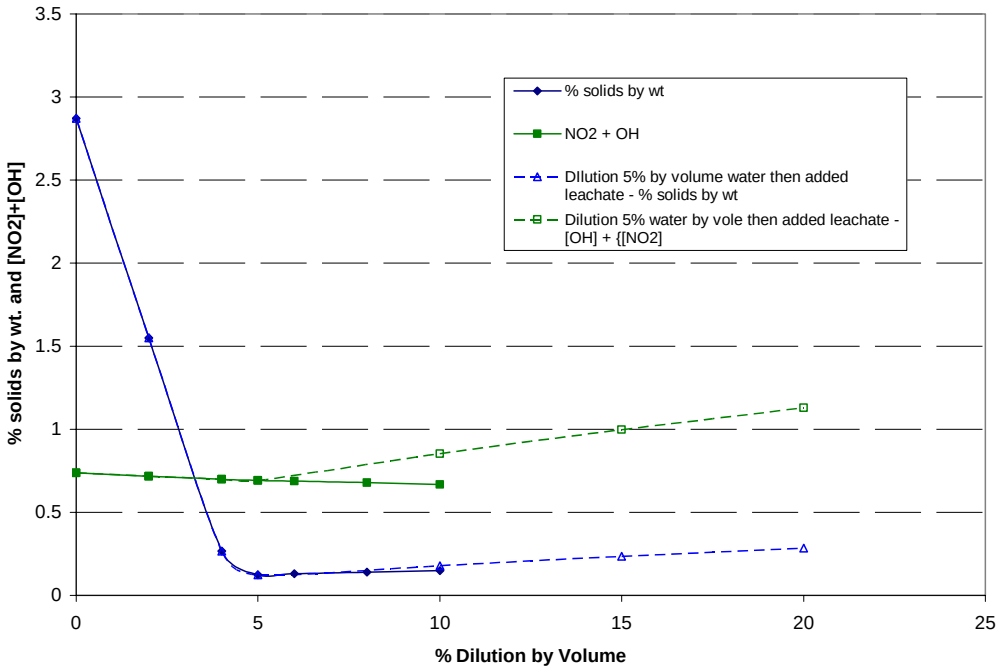

Figure 7. Initial water dilution results for transfer stream 4 followed by the addition of the Batch 5 leachate stream to attain corrosion protection.

The percent dilution by volume of water curve was then used to determine the approximate dilution necessary to minimize the percent solids by weight. If the sum of the hydroxide and nitrite concentrations was less than 1.1 then the Batch 5 leachate was added to make the stream attain corrosion compliance. Addition of the leachate volume continued until [OH] + [NO2] =1.1M.

The main cause for the increase in the percent solids by weight during leachate addition, Figure 7, is from further reprecipitation of gibbsite, Table 8. The final predicted value for the solids loading remained below 0.3% by weight.

All of the transfer streams contained within Table 8, with the exception of streams 8-10, were evaluated according to the flowsheet in Figure 7. The results are given in Figure 8 where data for the extended dilutions using water are not shown.

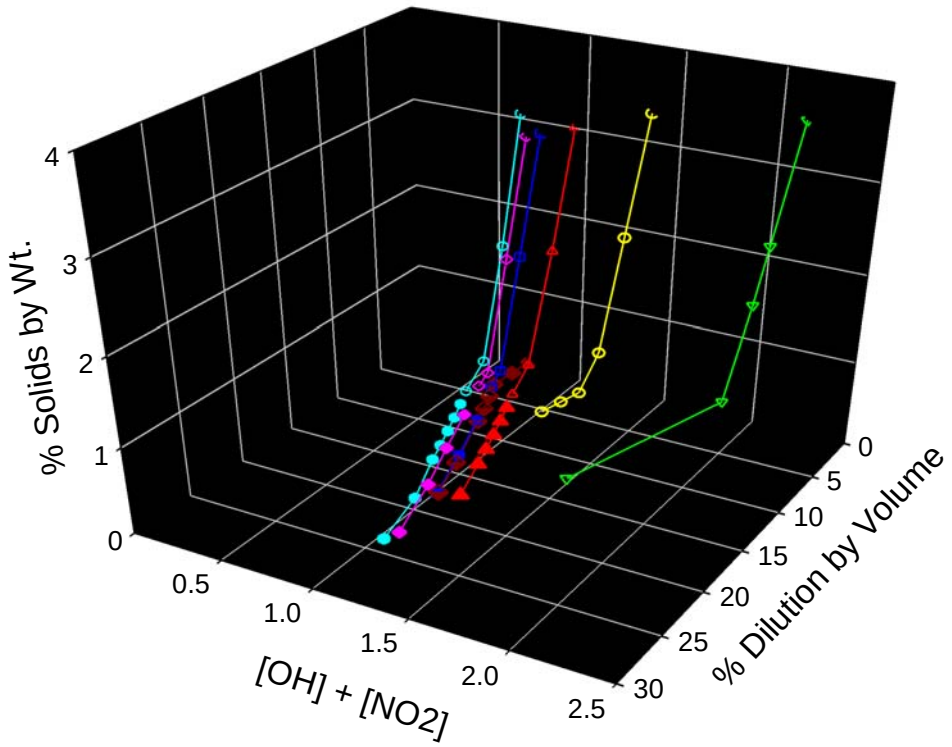

Figure 8. Plot of the percent solids by weight and the sum of the nitrite and hydroxide concentration against the percent dilution by volume for transfer streams 1-7. Transfer stream 1 is in green and the given streams can be counted from right to left.

Saltcake dissolution compositions obtained during the first and second dilution using the DWPF recycle stream will be within corrosion specifications solely with water dilution. At dilution stages 3 and greater, some fraction of the Batch 5 leachate must be used to

attain an [OH] + [NO_2] value of 1.1M. At larger initial percent by weight dilution of the saltcake, more of the anions are less saturated tending to lower the ionic strength and, more importantly, the hydroxide and nitrite concentrations are considerably lower. More of the Batch 5 leachate will have to be added to those streams processed later in the initial saltcake dissolution.

Figure 9 compared the processing of transfer stream 4 with water and leachate (green) and with leachate only (red). At 5 percent dilution by volume the main importance of adding water is that most all of the reprecipitated solids are dissolved, whereas, the solids dissolution with only the leachate takes a considerably larger dilution of around 10% to achieve a similar loading. At the end of the leachate addition, however, the overall percent solids by weight are approximately the same, still processing of the lower solids loading stream should be preferable. .

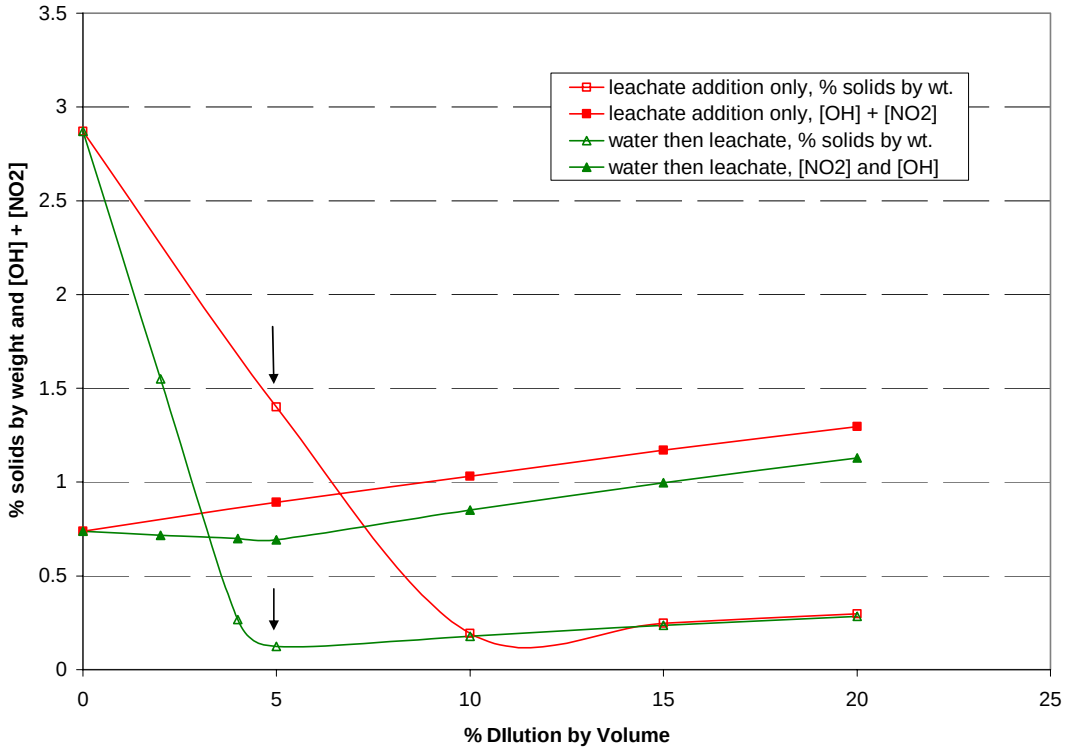

Figure 9. Processing of transfer stream 4 from saltcake dissolution of the waste in SRS tank 25F. The green data points represent the initial addition of water followed by the addition of leachate and the red data points indicate the use of the Batch 5 leachate only.

WORK FORECAST

The remaining samples, PXX655 and HB-XX-025 (emulsion) are currently undergoing analysis for solids and the aqueous portions. A final letter report will be sent to site personnel upon completion.

A considerable amount of data has been generated through the simulations presented here and those presented earlier for the Tanks 25F waste. These results will be compiled into a separate letter report for comments by engineers at SRS. Additional calculations are

being developed to assess the processing of the transfers streams within the CSSX system. Specifically, there are 2 process steps where nitric acid is used. The interaction of the acid with these basic streams may result in the formation of additional solids or changes in heat transfer and thermal loads that should be considered in specifying the waste acceptance criteria for the CSSX facility.

CONCLUSIONS

Analyses performed on five, as received, solid samples have been completed and results presented. All solids investigated to date were determined to be some form of an aluminosilicate compound with trace amounts of iron oxide and gibbsite or small amounts of sodium components found within the simulant. The results obtained in XRD were confirmed with ICP analysis of the digested solids and were found to be in good agreement.

Additional calculations have been reported on the processing of the waste from tank 25F to generate feed for the CSSX process. It was found that the use of water can initially reduce solids loadings and addition of the DWPF Batch 5 leachate can impart corrosion protection to the tanks containing these streams. This amounts to a re-use of the caustic that was originally added to Batch 5 to reduce aluminum loadings and a need not to add addition NaOH to the tank waste. More leachate is necessary for streams taken later in the saltcake dissolution process. The approach using both water and leachate addition has benefits in solids loading control.

REFERENCES

1. Dimenna, R.A.; Elder, H.H.; Foweler, J.R.; Fowler, R.C.; Gregory, M.V.; Hang, T.; Jacobs, R.A.; Paul, R.K.; Pike, J.A.; Rutland, P.L.; Smith, F.G.; Subosits, S.G.; Taylor, G.A.; Campbell, S.G.; Washburn, F.A. “Bases, Assumptions, and Results of the Flowsheet Calculations for the Decision Phase Salt Disposition Alternatives” WSRC-RP-99-00006, Rev. 3, Westinghouse Savannah River Company, Aiken, SC (2001).
2. Leonard, R.A.; Aase, S.B.; Arafat, H.; Conner, A.C.; Chamberlain, D.B.; Falkenberg, J.R.; Regalbutto, M.C.; Vandergrift, G.F. “Experimental Verification of Caustic-Side Solvent Extraction for Removal of Cesium from Tank Waste” *Sol. Extr. and Ion Exch.* **21(4)**, *2003*, 505.
3. Campbell, S.G.; Geeting, M.W.; Kennell, C.W.; Law, J.D.; Leonard, R.A.; Walker, D.D. “Demonstration of Caustic-Side Solvent Extraction with Savannah River Site High Level Waste” WSRC-TR-2001-00223, Rev.1, Westinghouse Savannah River Company, Aiken, SC (2001).
4. Weber, E.J. “Aluminum Hydroxide Dissolution in Synthetic Sludges” DP-1617, 1982.
5. Hay, M.S.; Pareizs, J.M.; Bannochie, C.J.; Stone, M.E.; Click, D.R.; McCabe, D.J. “Preliminary Data from the 3L Tank 51H Aluminum Dissolution Test” SRNL-CST-2007-00102, Savannah River National Lab, Aiken, SC (2007)
6. Ketusky, E., “High Level Waste System Impacts from Acid Dissolution of Sludge”

CBU-PIT-2005-00260R1, Westinghouse Savannah River Company, Aiken, SC (2005).
7. Fox, L., "CSTF Corrosion Control Program," WSRC-TR2002-00327, Rev. 3, Westinghouse Savannah River Company, Aiken, SC (2003).
8. Waste Acceptance Criteria for Aqueous Waste sent to the Z-Area Saltstone Production Facility (U). X-SD-Z-00001, Rev. 2, 2004.
9. Fahr; M. Bassett; and M. Brugh. CSSX Dispersion (Emulsion) Test, Milestone Progress Report, April, 2008.
10. Lindner, J. S. and L. T. Smith, "Modeling and Experimental Support for High Level SRS Salt Disposition Alternatives," in Accelerating Cleanup of the Defense Nuclear Legacy, Report No.07040R02, Institute for Clean Energy Technology, Mississippi State University, 2008, p(3).
11. Martino, C. J., et al., "Analysis and dissolution testing of tank 25F core samples (FTF-504-513)," WSRC-STI-2007-00123, Rev.0, Savannah River National Laboratory, Aiken, SC, (2007).

Task 2

Process Improvements for the Defense Processing Facility (DWPF)

Jagdish P. Singh

INTRODUCTION

An on-line, real-time analysis of Defense Waste Processing Facility **(**DWPF) samples will significantly increase analytical throughput and will reduce waste generation in radiological analytical facilities. The goal of this Task is to develop system for rapid analysis of DWPF samples to accelerate waste processing using laser-induced breakdown spectroscopy (LIBS).

The first subtask of this project will provide a system for direct analysis of slurry in the DWPF's analytical shielded cells. The capability of direct analysis of slurry will significantly increase analytical throughput and will reduce waste generation in radiological analytical facilities, providing analyses suitable for waste acceptance and production records. The second subtask is to provide compositional data for plutonium residue feeds before being processed into glass.

LIBS uses a high pulse energy laser beams to produces a micro plasma to vaporize, dissociate, excite, or ionize species on material surfaces. The study of the atomic emission from the micro plasma provides information about the composition of the material. LIBS is a powerful analytical tool which is suitable for quick and on-line elemental analysis of any phase of material.[1-4] The laser light and emitted signal can be delivered via optical fiber so it is useful for hazardous situations. LIBS can provide an accuracy of 3-5% for elements with concentration >1% and an accuracy of 5-10% or better for minor elements in solid samples.

WORK PERFORMED

LIBS experiments of DWPF slurry continued by direct sampling the slurry in a small beaker. Figure 8 shows a general schematic diagram of the experimental setup used for recording LIBS spectra of DWPF slurry. A frequency-doubled, Q-switched Nd:YAG laser was incorporated into the LIBS system as an excitation source. The 532-nm laser light is focused onto the sample surface using an ultraviolet grade quartz lens of 500 mm focal length. Atomic emission from the laser-induced plasma was collected by an optical fiber bundle using a UV-grade quartz lens and sent to an Echelle spectrograph with

1024×1024 element intensified charge coupled device. To avoid slurry sedimentation, the sample is continuously stirred by magnetic stirrer during the LIBS measurement. Different stirring speeds were tested to obtain the proper speed that will have less sample surface disturbance and most reproducible LIBS signal. Different amounts of chemical were added to DWPF slurry in order to record calibration data. We found some added chemical did not mix well with the original sample even though the sample is stirred during the measurement. This problem will need carefully examined to find proper solution.

For quantitative LIBS analysis, elemental concentrations are commonly measured by using calibration curves which are obtained from the intensity of an analyte line at different concentrations of a species. This method can provide accurate results, if the measured signal only arises from one source (i.e. the concentration of analyte species). The selection of the analyte lines for univariate calibration also plays an important role for predicting the concentration from unknown samples. This univariate calibration curve can be a very effective method for similar matrix and the measured concentration is in linear range of the calibration curve. However, it will not give accurate results for a different matrix sample or analyte lines with spectral interference (e.g. self-absorption) if proper correction factors are not applied to the calibration curves. Recently, multivariate calibration method such as Partial Least-Squares (PLS) regression and Artificial Neural Networks (ANN) have been applied to LIBS analysis of different samples.[5-7] Unlike univariate calibration, where only one spectral line is used for calibration, multivariate calibration take into account many spectral lines and use a weighted average of all the measurements in data processing to minimize the influence of the noise and spectral interference. Multivariate calibration also allows outliers to be detected. Deviations can arise from instrument errors and sampling errors.

In this work period, we have evaluated the use of PLS to LIBS analysis of slurry sample. Partial least square is a quantitative spectral decomposition technique that is closely related to Principal Component Regression (PCR).[8,9] PCR first decomposes X-variable (e.g. sample spectral data) into a set of eigenvectors and scores, and regresses these against the Y-variable (e.g. sample composition) as a separate step. PLS performs single step decomposition in both the X variables and Y variables. It uses the correlation relationship between the X- and Y- variables to decompose the variables into their most common variations. PLS generates two sets of vectors and two sets of corresponding scores: one for the X-, and the other for the Y-variables. The two sets of scores are related to each other through regression, and a calibration model is then constructed. Our optimized models were obtained by the “leave one out” cross-validation technique based on the minimum predicted residual sum of squares (PRESS). The predictive quality of the models was evaluated by calculating the standard error of cross validation (SECV) and the standard error of prediction (SEP) in the validation step with independent samples. In this work, PLS was performed with GRAMS/AI 7.02 PLSplus/IQ (Thermo Galactic, Salem NH). The univariate calibration curves for Si and Na in slurry are shown in Figure 9. The calibration curve for Si has reasonable good linear correlation coefficient however; the standard deviation of the measurement is large. Due to spectral interference, it is not easy to find a Na line for analysis. The resonance line suffers from self-absorption and other lines contain interference from spectral lines of other species. The

calibration curve of Na shows poor linear correlation coefficient and large standard deviation. The PLS analysis results of Si and Na using the same calibration data set that used in univariate calibration are shown in Figure 9. Unlike univariate calibration, it use one data per spectrum (i.e. the intensity area ratio of an analyte line with a reference Al line), the PLS use 4860 data points per spectrum in data processing. It is clear from Figure 10, the predicted value are in close agreement with the true value even the difficult species like Na. Improved standard deviations were also found in PLS analysis.

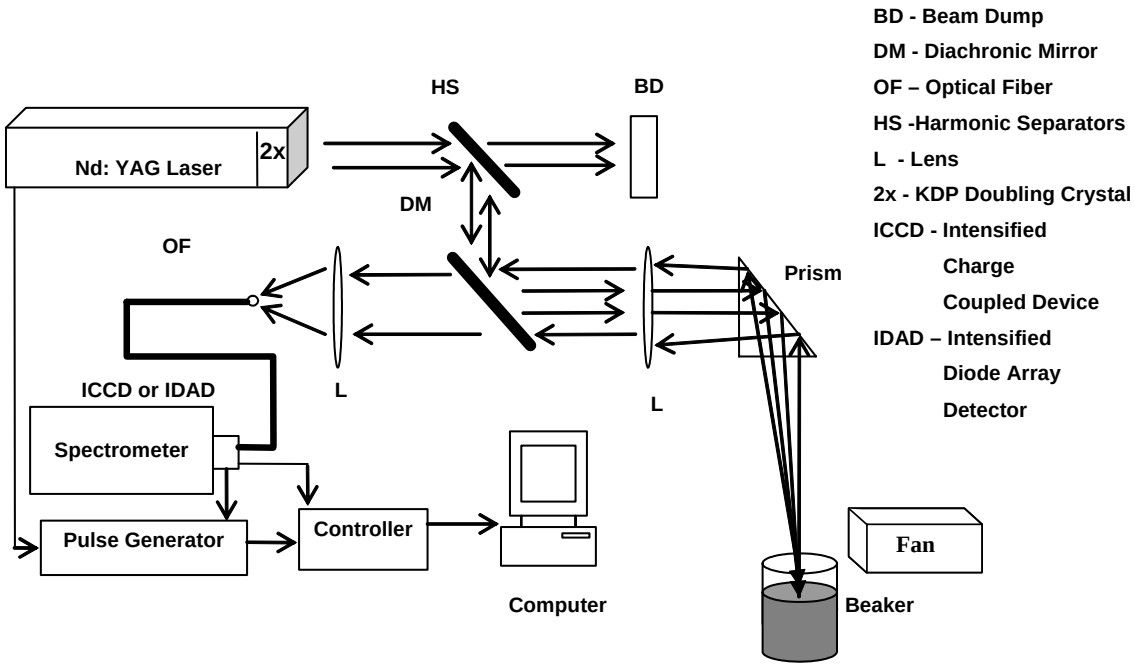

Figure 10. LIBS experimental setup for direct slurry sampling.

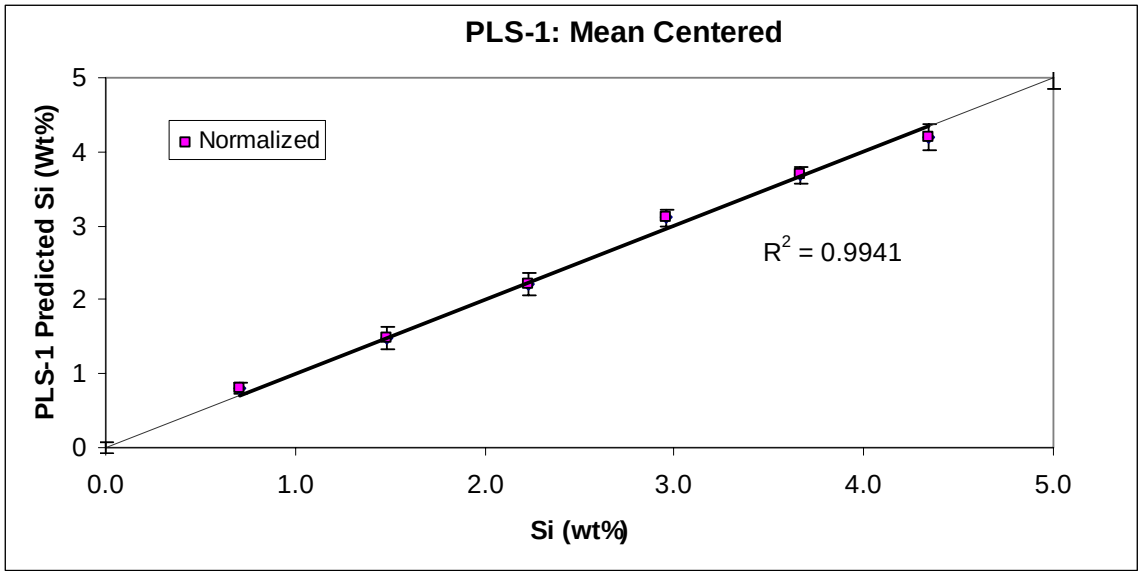

Figure 11. LIBS slurry Analysis using univariate calibration based on Intensity Ratio.

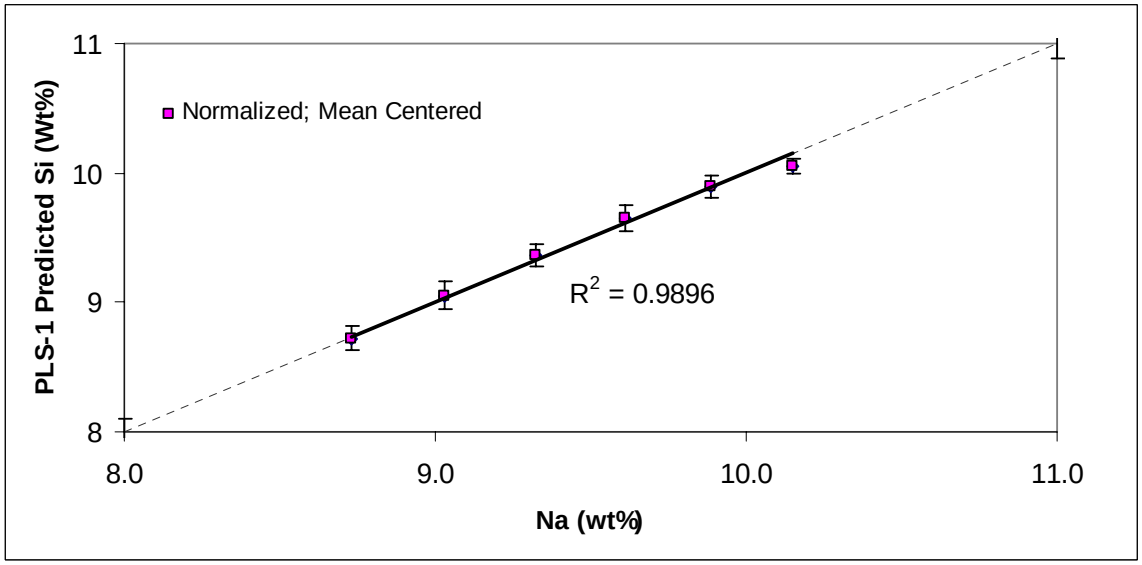

Figure 12. LIBS slurry analysis using partial least square.

WORK FORECAST

The work to improve the performance of slurry measurement with both different sampling methods and data processing techniques will continue. A compact spectrometer will be used to record DP-LIBS data of solid and liquid samples.

CONCLUSION

In order to improve the performance of direct slurry sampling, various experimental configurations and experimental parameters were evaluated to obtain the optimized experimental condition. Calibration data for direct slurry sampling were recorded by addition of various amount of chemical into the slurry. Two data analysis methods were tested with the recorded calibration data. The PLS analysis give much improved analytical performance as compared to univariate calibration.

REFERENCES

1. J. P. Singh and S. N. Thakur, Laser- Induced Breakdown Spectroscopy, Elsevier Science B. V., Amsterdam, The Netherlands, 2007.
2. A. Miziolek, V. Palleschi and I. Schechter, Laser Induced Breakdown Spectroscopy (LIBS): Fundamentals and Applications, Cambridge University Press, 2006.
3. Fang-Yu Yueh, Jagdish P. Singh and Hansheng Zhang, "Laser-induced breakdown spectroscopy-elemental analysis", in *Encyclopedia of Analytical Chemistry*, R.A.Meyers, ed. (Wiley, New York, 2000).
4. Celio Pasquini; Juliana Cortez; Lucas M. C. Silva; Fabiano B. Gonzaga "Laser Induced Breakdown Spectroscopy, J. Braz. Chem. Soc. 18(3), 463 (2007).
5. J.B. Sirven, B. Bousquet, L. Canioni, and L. Sarger, "Laser Induced Breakdown Spectroscopy of Composite Samples: Comparison of Advanced Chemometrics Methods", Anal. Chem. 78, 1462 (2006).
6. M. Z. Martina, N. Labbéb, T. G. Rialsb and S. D. Wullschlegera, "Analysis of preservative-treated wood by multivariate analysis of laser-induced breakdown spectroscopy spectra" , Spectrochimica Acta Part B: Atomic Spectroscopy, 60 (7-8), 1179 (2005).
7. B. Bousquet, J.-B. Sirven, L. Canioni, "Towards quantitative laser-induced breakdown spectroscopy analysis of soil samples", Spectrochimica Acta B 62, 582 (2007).
8. K. H. Esbensen, Multivariate Data Analysis in Practice, 5th edition, Camo Inc., 2004.
9. Duran Meras I.; Munoz de la Pena A.; Rodriguez Caceres M.I.; Salinas Lopez F., "Simultaneous fluorometric determination of nalidixic acid and 7-hydroxymethylnalidixic acid by partial least squares calibration", 45(5), 899 (1998).

Task 3

High Efficiency Particulate Air (HEPA)

Rangaswami Arunkumar, Charles A. Waggoner

INTRODUCTION

The Institute for Clean Energy Technology (ICET) at Mississippi State Univeristy (MSU) has been involved in evaluating the performance of AG-1 HEPA filters for several years. A number of 12”x12”x11.5” filters have been loaded with a variety of aerosol challenges that include potassium chloride (KCl), iron salts, and soot. Filter testing has involved different media velocities and particle size distributions of the aerosol challenge. Work began on developing the methodology for autopsying selected filters from this group during the 2nd quarter of 2008. Such a procedure would enable ICET researchers to evaluate loading patterns associated with testing that has been conducted at ICET by methodically disassembling loaded filters.

WORK ACCOMPLISHMENT

An AG-1 12”x12”x11.5” filter loaded over the course of three days in 2003 from 1” w.c. to 6” w.c. with potassium chloride was autopsied during the third quarter of 2008. Autopsy procedures were performed on a number of pleats within this filter. Five such pleats were chosen for autopsy into a 5x5 grid pattern producing 50 small coupons from each pleat. The pleats chosen were the left edge, left center, center, right center, and right edge of the filter. Analysis of the mass loading on each of these sections yielded the results depicted in Figure 13.

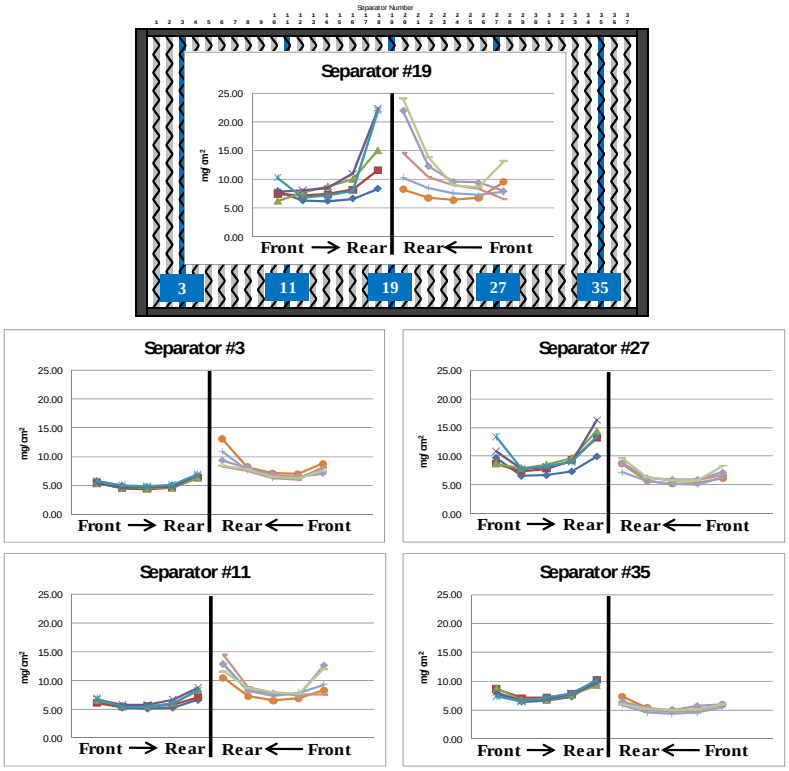

Figure 13. Results of Autopsy into 5x5 Grid Sections.

These results show an increased mass loading of the sheet of filter media closer to the center of the filter. The consistent pattern of media on the mid-line side of a separator having a larger loading is consistent with observations of build-up on the protective wire screen. Figure 14 provides a close-up view of KCl captured on the wire screen. This pattern appears indicative of an angular component to the air flow and is radially symmetrical around the center of the filter face. It is also significant to note that maximum loading rate is observed to occur on the mid-line pleat.

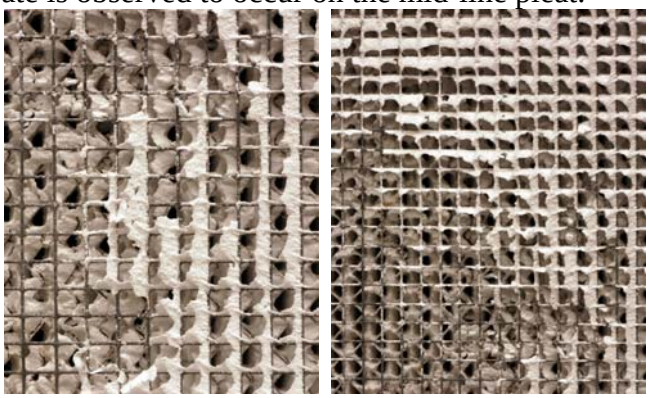

Figure 14. Close-up View of KCl on Wire Screen.

Three presentations were made by ICET researchers at the Nuclear Air Cleaning Conference in Seattle, WA. These presentations were entitled “Filter Autopsy for Evaluating Effects of Particle Size Distribution and Media Velocity on Loading Patterns”, “The Effects of Media Velocity and Particle Size Distribution on Most

Penetrating Particle Size and Filter Loading Capacity of 12”x12”x11.5” AG-1 HEPA Filters”, and “Section FI Overview and Status Report”.

WORK FORECAST

ICET took part in the Program Advisory Committee (PAC) meeting for Waste Management ’09 (WM09) in Phoenix, AZ. Abstracts were reviewed and sections/assignments were made for both oral presentations and poster sessions. The session will be held on Tuesday morning of the conference the first week of March 2009.

Task 4

Support of Hanford Single Shell Tank Waste Disposition

Jeffrey Lindner, John Luthe, Larry Pearson, Laura Smith, Rebecca Toghiani

INTRODUCTION

Knowledge of the chemistry associated with the wastes contained in the Hanford tank farms has bearings on waste pretreatment, retrieval, vitrification, alternative processing, and tank closure operations. Much of the work conducted at ICET has focused on developing an understanding of the salt chemistry found in these tanks. A number of experiments have been performed and have led to the development of the V7DBLSLT thermodynamic database for use in the OLI Systems Inc. Environmental Simulation Program (ESP). This work consisted of extensive solubility measurements of specific sodium salt systems at the temperatures and pH values typical of the site waste [1,2]. Additional efforts were directed at aluminum chemistry and with development of a neural network model based on a framework of ESP simulations for use in conjunction with the Hanford H2 (overall campaign flowsheeting) simulator.

The Hanford Tank Waste Operations Simulator (HTWOS) is used for scheduling the entire retrieval campaign and includes model representations for vitrification and low activity waste processes. Chemistry representations used in HTWOS rely on wash and leach factors as opposed to direct, solid-liquid equilibrium thermodynamic calculations. Site engineers have previously requested an evaluation of the feasibility of upgrading the chemistry representation to include ESP. Having a proper chemistry representation within HTWOS will reduce the uncertainties associated with wash and leach factors. Earlier work identified the use of a neural network as a preferred option due to the large number of calculations needed during a HTWOS campaign run. As an initial evaluation of this approach, site engineers requested the application of the process to the retrieval of C farm tanks.

The development of a neural network for use within the HTWOS model requires an extensive set of training data. To generate this data, ICET constructed an ESP program process model of the retrieval of C tank waste based on the procedures and constraints followed in the Modified Sluicing Method [3] of waste retrieval. With this ESP simulation framework, a neural network training set consisting of the input stream values

and the ESP computation output can be built. Construction of the training set to cover the ranges of possible input streams requires an execution of the ESP program for each case. Since ESP is an interactive program, a batch mode processing routine is necessary to replace the ESP user interface. Perl [4], a freely available platform independent programming language was used to provide this batch mode processing. The retrieval of C-108 waste using flush liquid from AN-106 was simulated with the ESP program process model and Perl to provide the initial neural net training data. Simulations of each of the remaining C farm tanks, using this model, will provide the data necessary for the generation of an expanded neural network training set applicable across the entire range of C farm tank compositions. This expanded neural network will allow an evaluation of the retrieval schedule including different combinations of source and destination tanks. Since the neural network utilizes equilibrium chemistry as its basis, the potential result is a more accurate, as well as, timely method for Hanford campaign simulation.

WORK ACCOMPLISMENT

The retrieval of waste from the Hanford C farm tanks is currently scheduled to utilize two waste recovery techniques. The Modified Sluicing with Recycle method (MSwR) has been selected for use in the majority of tanks. This method has been modeled using the OLI ESP equilibrium program as reported previously [3, 5].

The retrieval of C farm tanks C-104, C-112, and C-111 will make use of both techniques. C-104 and C-112 are scheduled for use of the MSwR method while C-111 will be retrieved using the MRS method. The sequence of the retrievals is C-104 followed by C-112 and then C-111. The destination tank for each of these C tanks is AN-101. Modeling of each tank retrieval was performed utilizing the OLI ESP equilibrium program to be consistent with the prior MSwR and MRS simulations. The basic structure of the MSwR model was maintained as a four-stage process with constraints as previously reported [3]. The MRS model consists of two stages with constraints also previously reported [5].

Table 9 displays several parameters of AN-101 during the complete retrieval of the C tanks. These same parameters for the flush stream that is returned to the AN tank are also displayed. The stage numbers correspond with each stage of the process with the initial state listed as stage 0. Figures 15 and 16 display several of these parameters in chart form. Figures 17 and 18 graphically show conditions of the flush stream that is returned to AN-101.

Table 10 shows the amounts of several of the major solids, which are collected and appear in AN-101. Again, these solids are shown after each stage of the total retrieval process. Figures 15 and 16 show these major solids in chart form.

Table 11 shows the conditions present in each of the C tanks during the retrieval process. Again, stage 0 is used to represent the initial conditions in the tank.

Table 9 – AN tank and flush conditions during retrieval of C-104, C-112, and C111

			C-104				C-112				C-111	
AN-101 Tank conditions	stage	0	1	2	3	4	5	6	7	8	9	10
	gallons	1,142,807	1,161,880	1,533,492	1,609,493	1,744,139	1,749,533	1,822,602	1,865,976	1,920,537	1,944,238	2,028,836
	specific gravity	1.35	1.35	1.33	1.33	1.31	1.30	1.31	1.31	1.30	1.30	1.30
	wt% solids	3.74	3.66	6.59	6.92	6.72	6.37	7.16	7.32	7.30	6.88	7.73
	vol% solids	2.33	2.22	3.51	3.62	3.44	3.16	3.62	3.68	3.65	3.28	3.70
	Na molarity	7.53	7.44	6.49	6.23	5.79	5.78	5.69	5.60	5.46	5.60	5.44
	pH	14.28	14.27	14.12	14.09	14.02	14.01	13.96	13.94	13.92	13.89	13.84
	wt% water	56.73	57.26	59.66	60.53	62.57	62.89	62.52	62.79	63.43	63.84	63.94
Flush return to AN-101	stage		1	2	3	4	5	6	7	8	9	10
	gallons		39,097	574,443	253,526	558,265	25,757	141,860	149,257	292,696	34,745	580,703
	specific gra		1.24	1.30	1.25	1.23	1.27	1.31	1.25	1.22	1.29	1.25
	wt% solids		2.20	9.99	4.40	1.19	2.44	9.99	4.40	1.19	9.34	4.17
	vol% solids		0.98	4.67	1.97	0.52	0.94	4.64	1.91	0.48	4.38	1.93
	Na molarity		4.97	4.95	4.90	4.96	5.00	4.91	4.66	4.80	3.57	4.99
	pH		13.93	13.91	13.84	13.85	8.65	11.92	13.56	13.77	6.27	13.65
	wt% water										64.29	68.27

Table 10 – AN-101 Solids during the Retrieval of C-104, C-112, and C-111

AN-101 Solids		C-104				C-112				C-111	
stage	0	1	2	3	4	5	6	7	8	9	10
Total gmoles	1,970,417	2,008,520	4,622,989	5,124,296	5,447,069	5,502,617	5,912,425	6,101,187	6,204,380	6,485,485	7,643,306
ALOH3	1,910,563	1,945,526	4,076,046	4,484,419	4,755,978	4,797,557	5,013,089	5,111,873	5,167,017	5,354,719	6,257,188
BIOH3							1,625	3,082	3,913	4,908	11,357
CROH3	29,738	30,011	48,311	51,848	54,230	54,481	55,968	56,685	57,095	58,681	59,238
FEIIIOH3			309,051	370,690	411,839	418,628	509,475	552,726	577,354	609,084	805,177
NIOH2	5,896	6,308	35,452	41,078	44,801	47,590	93,014	114,667	126,968	182,057	212,065
FAPATITE	1,968	2,105	11,806	13,678	14,917	16,023	36,232	45,866	51,338	53,975	70,401
NA2C2O4	21,847	23,053	62,043	67,095	59,759	60,286	59,904	56,454	51,365	49,402	40,552
NAALCO3OH2											
UIVO2	405	1,517	80,282	95,487	105,545	108,053	143,118	159,834	169,329	172,658	187,329

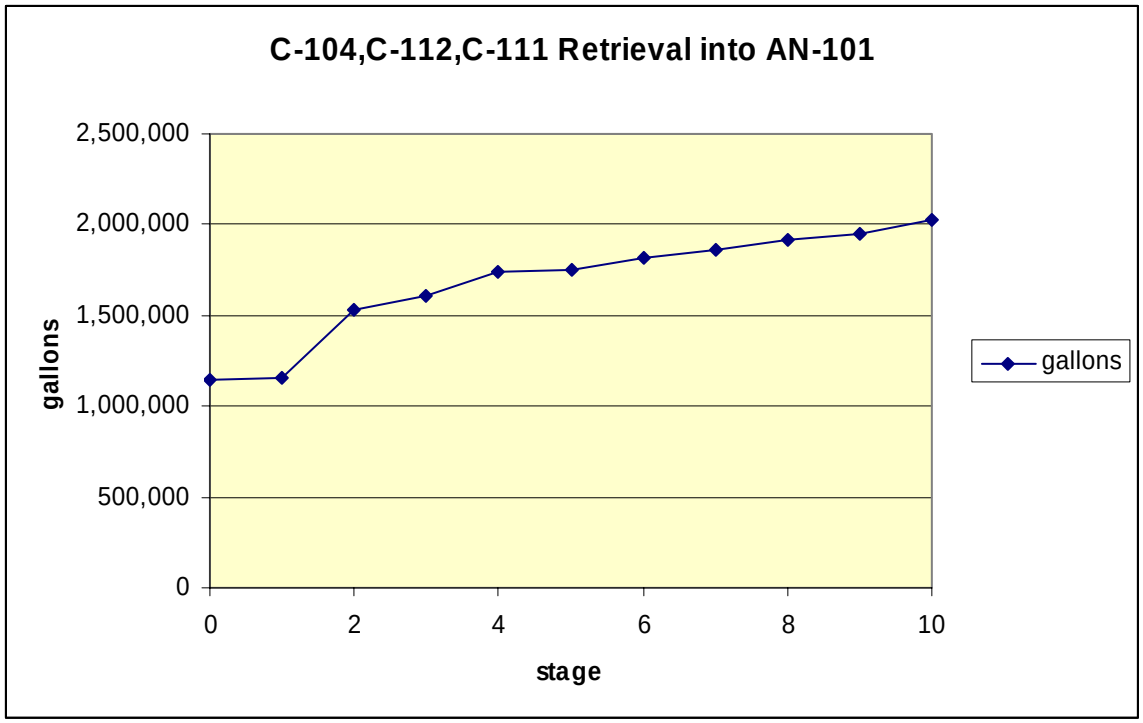

Figure 15 – Total Volume of AN-101 During Retrieval of C tanks

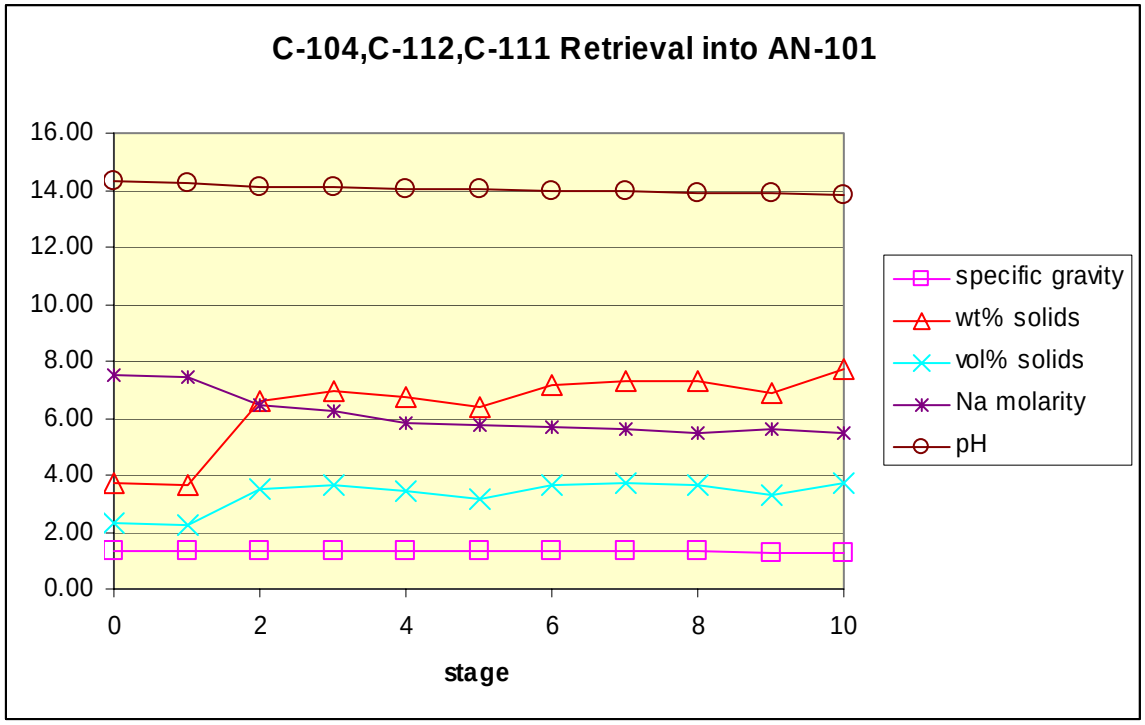

Figure 16 – AN-101 Conditions During Retrieval of C tanks

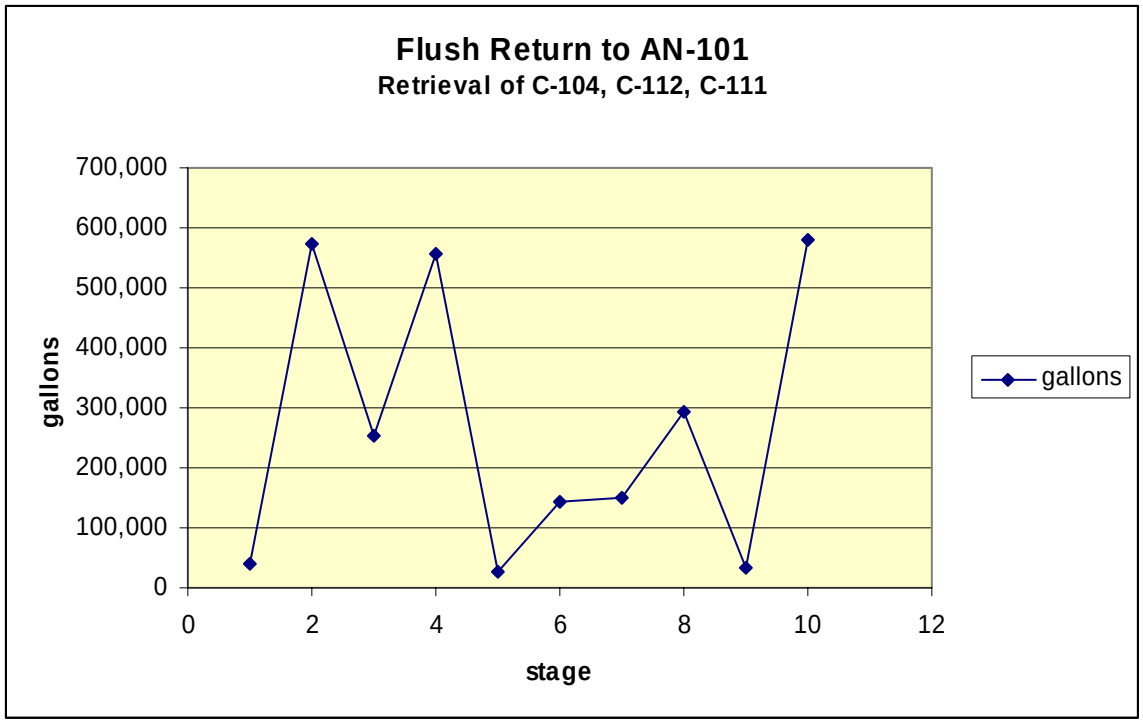

Figure 17 – Total Volume of Flush Stream to AN tank

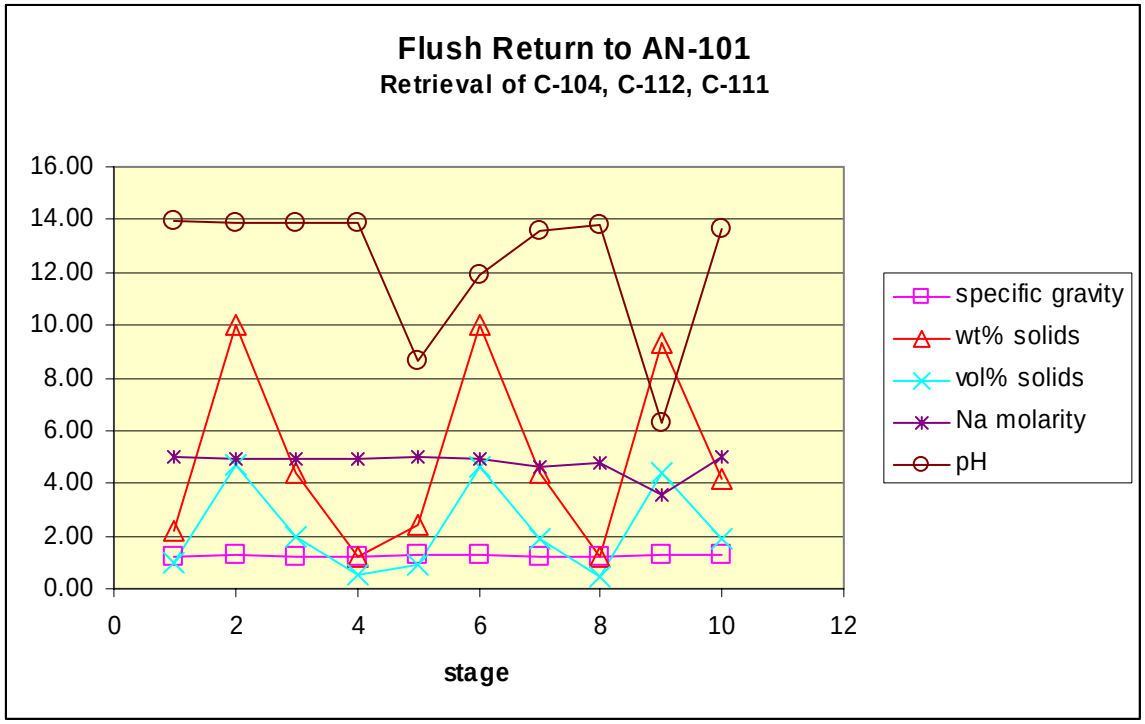

Figure 18 – Conditions of Flush Stream to AN tank

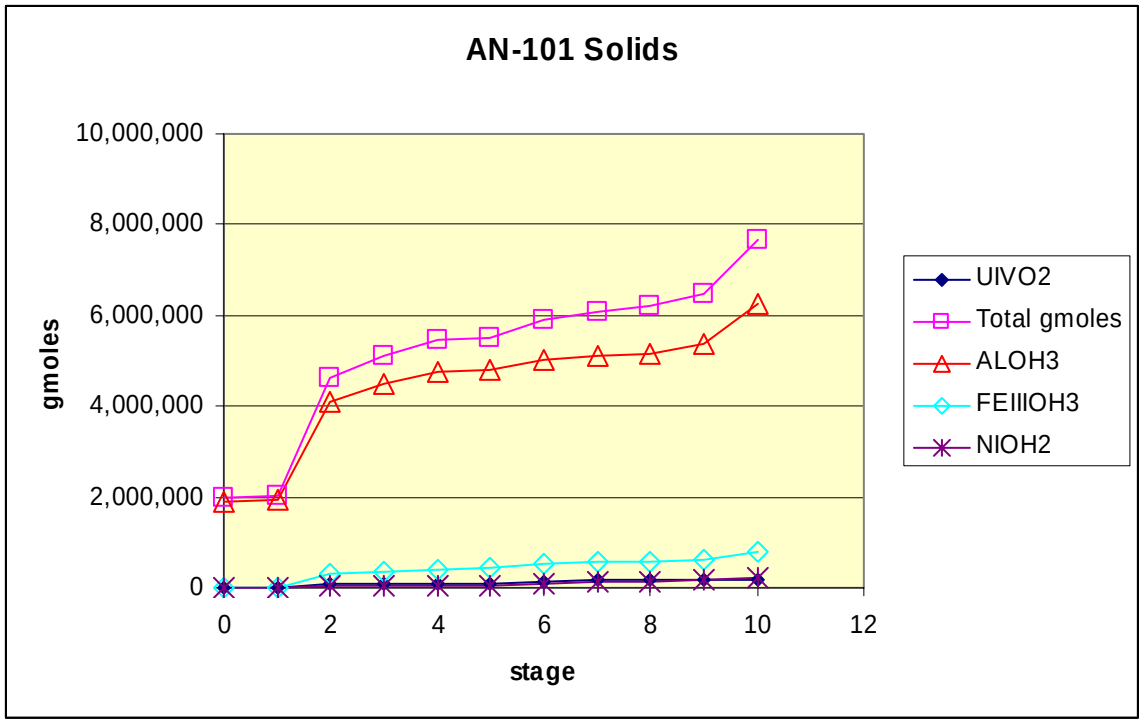

Figure 19 – AN-101 Solids (gmoles)

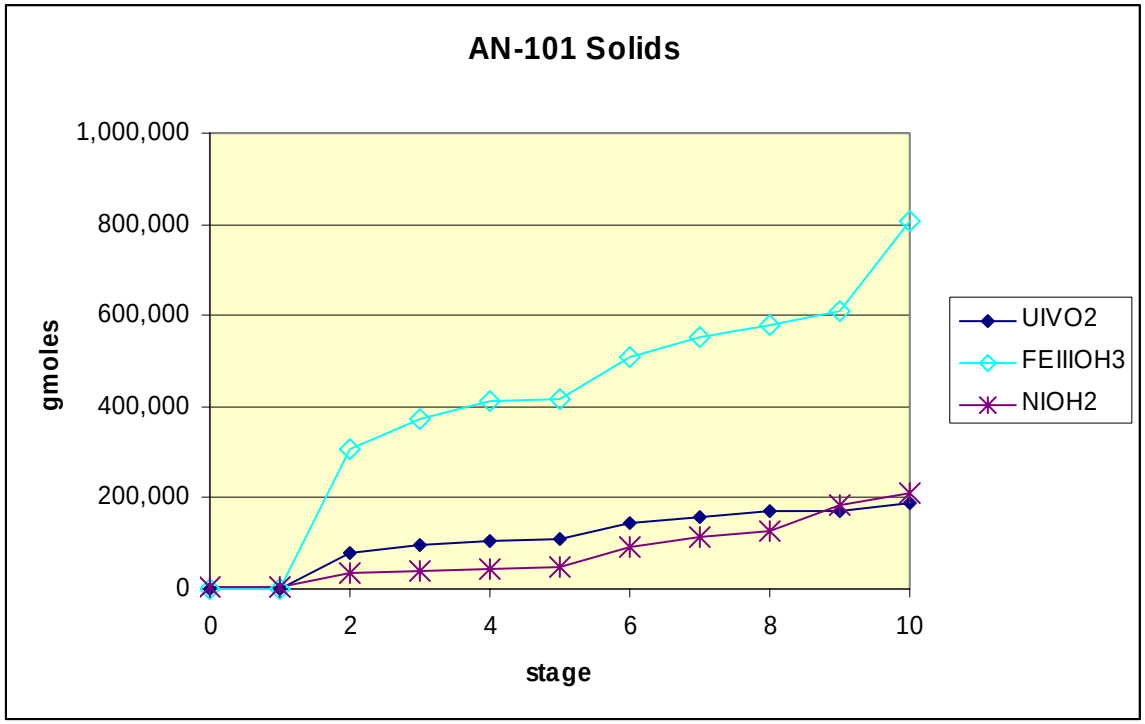

Figure 20 – AN-101 Solids (gmoles)

Table 11 – C tank Conditions During Retrieval Into AN-101

	stage	0	1	2	3	4
C-104 Tank conditions	gallons	304,551	299,020	19,908	8,323	2,731
	specific gravity	1.43	1.43	2.06	2.20	2.19
	wt% solids	24.62	24.80	72.03	79.35	78.59
	vol% solids	12.63	12.71	53.22	62.71	61.55
	Na molarity	4.23	4.48	2.77	2.09	1.92
	pH	13.93	13.93	13.93	13.89	13.89

	stage	0	1	2	3	4
C-112 Tank conditions	gallons	99,015	93,547	19,644	8,014	2,568
	specific gra	1.44	1.45	1.80	1.91	2.29
	wt% solids	20.99	22.74	55.00	63.28	78.33
	vol% solids	9.17	10.05	34.91	42.21	59.08
	Na molarity	4.45	5.17	3.61	3.11	2.35
	pH	6.69	8.65	11.99	13.58	13.80

	stage	0	1	2
C-111 Tank conditions	gallons	54,090	30,207	2,592
	specific gra	1.62	1.85	2.20
	wt% solids	43.36	61.42	81.11
	vol% solids	25.55	41.47	66.05
	Na molarity	3.15	3.57	4.99
	pH	5.59	6.27	13.69
	wt% water	39.85	27.36	13.46

WORK FORECAST

Additional ESP process simulations will be developed for the remaining C tank retrievals. In particular, the ESP simulation model will be used to evaluate C tank retrievals using both the modified sluicing (MSwR) and the mobile retrieval system (MRS) methods [3,5] as per the current Hanford retrieval schedule [5]. Neural network training set data will be generated using the expanded ESP process simulations. Additional batch scripting modules for the ESP program will be developed for stages of the process simulations, as needed to build the neural network training sets.

CONCLUSIONS

An ESP process simulation model, which approximates the C tank farm Modified Sluicing with Recycle (MSwR) and the Mobile Retrieval System (MRS) for waste retrieval has been used to evaluate the retrieval of C-104, C-112, and C-111 waste into AY-101. This ESP process model will be used to generate data to train a neural network representation of the C tank farm retrieval chemistry for use in HTWOS. Batch mode processing programs for ESP have been tested to generate single tank retrieval data for the neural network training set. Development has begun extending the programs to sequential multiple tank retrievals.

1. Toghiani, R. K., Phillips, V. A., and Lindner, J. S., "Solubility of Na-F-SO_4 in Water and in Sodium Hydroxide Solutions," Journal of Chemical and Engineering Data 50(5), 1615, (2005).

2. Selvaraj, D. K., (2003), Solubility Studies in the Na-F-PO_4 System in Sodium Nitrate and in Sodium Hydroxide Solutions, MS Thesis, Chemical Engineering, Mississippi State University, Mississippi State, MS.

3. Lindner, J.S., Luthe, J.C., Pearson, L.E., Smith, L.T., Toghiani, R.K., (2007), "Process Chemistry and Operations Planning for Hanford Waste Alternatives" in "Accelerating Cleanup of the Defense Nuclear Legacy," ICET Quarterly Technical Progress Report for the period July 1, - September 31, 2007, Report Number 07040R03 U. S. Department of Energy Agreement Number DE-FC01-06EW-07040, Mississippi State, MS.

4. Larry Wall, Tom Christiansen, Jon Orwant, "Programming Perl," Third Edition, O'Reilly, Sebastopol, CA 2000.

5. Lindner, J.S., Luthe, J.C., Pearson, L.E., Smith, L.T., Toghiani, R.K., (2008), "Process Chemistry and Operations Planning for Hanford Waste Alternatives" in "Accelerating Cleanup of the Defense Nuclear Legacy," ICET Quarterly Technical Progress Report for the period April 1, - June 30, 2008, Report Number 07040R06 U. S. Department of Energy Agreement Number DE-FC01-06EW-07040, Mississippi State, MS.

Task 5

Phytoremediation and Long-Term Monitoring of Heavy Metal Contaminants

Yi Su, Fengxiang Han, and David Monts

INTRODUCTION

Volatilization is a major process of Hg cycling from Hg contaminated soil and has proved to be am important pathway to plant uptake. Indian mustard and Chinese brake ferns have been recommended for phytoremediation of metal contaminated soils due to fast growth and high capability of uptake, respectively. However, the foliage uptake of Hg by these two plants has not been previously studied.

WORK ACCOMPLISHMENT

The experiments show, on average, that Indian mustard assimilated more Hg compared to Chinese brake fern under the same dose of Hg treatment and the same Hg source (Figure 13). In a chamber with 1 kg of Oak Ridge soil contaminated with 200 ppm Hg as $HgCl_2$, mercury concentrations in shoots of Chinese brake fern ranges from 40-90 mg/kg, while Indian mustard ranges from 75 to 120 mg/kg. The majority of Hg taken up by leaves of plants was accumulated in shoots with very limited transport into stem and roots (Fig. 13).

The Chinese brake fern, a hyperaccumulator plant for As, had a significantly high foliage uptake capability compared to Boston fern, a non-hyperaccumulator plant (Fig. 14). The chamber had 1 kg Oak Ridge soils contaminated with 1000 mg/kg Hg as $HgCl_2$. The experiments also show that foliage uptake from air increased with Hg load in air. Both ferns had higher foliage uptake of Hg from air equilibrated with $HgCl_2$ contaminated soils than HgS contaminated soils.

A very interesting observation was found in the chamber from Indian mustard, which had a much higher Hg concentration in air than from a chamber with brake fern (Fig. 15). This might be related to various factors including higher leaf Hg volatilization, and the effects of fast growth and higher biomass Indian mustard compared to a slow growth and lower biomass brake fern. Detailed mechanism requires further studies.

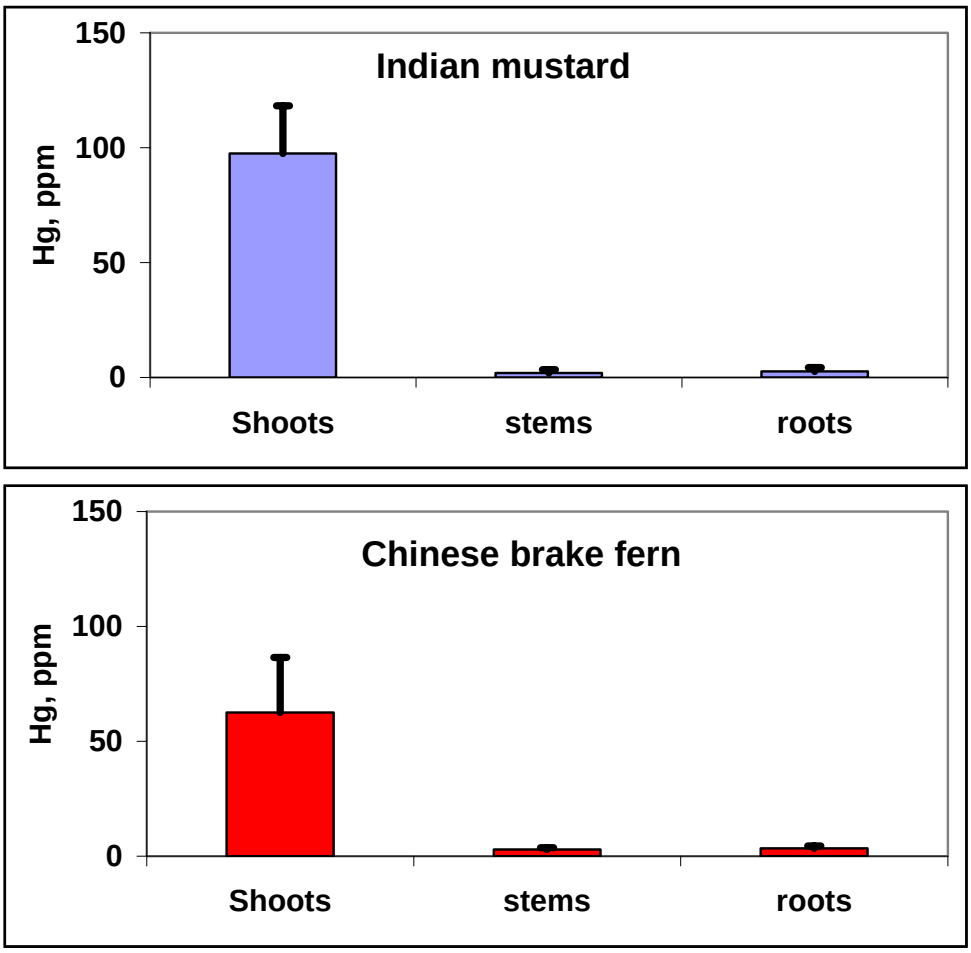

Fig. 21. Hg uptake by Indian mustard and Chinese brake fern from a chamber with 1 kg of Oak Ridge soils contaminated with 200 mg/kg HgCl2 and HgS.

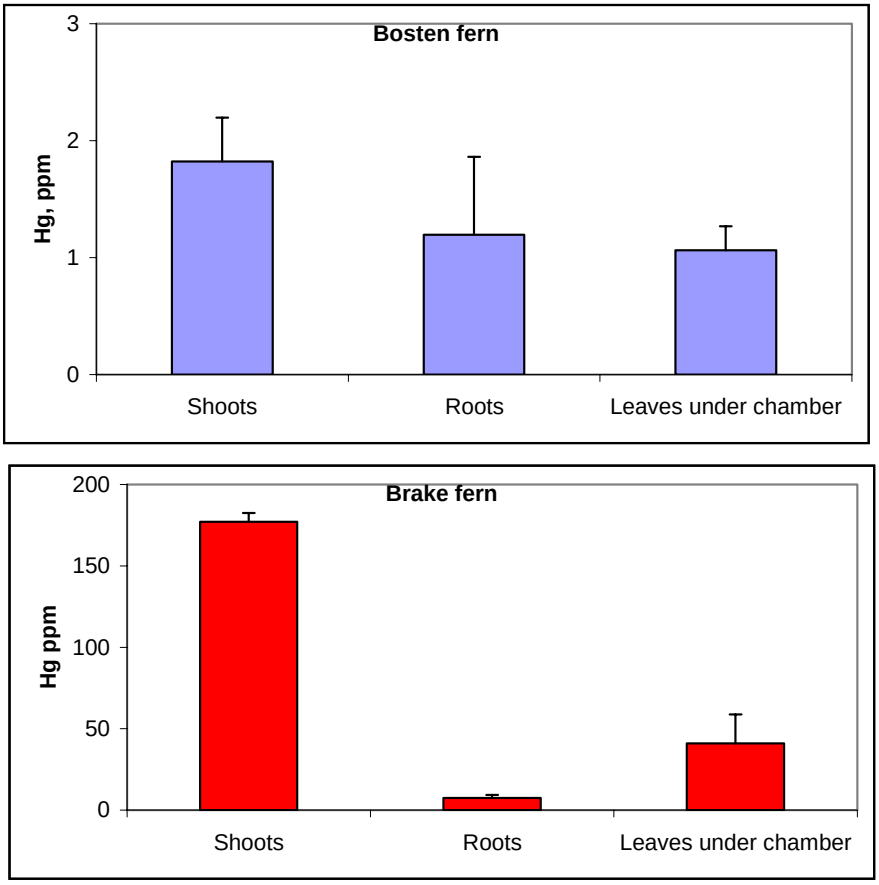

Figure 22. Hg uptake by two varieties of fern (Chinese brake fern and Boston fern) from a chamber with 1 kg of Oak Ridge soils contaminated with 1000 mg/kg $HgCl_2$.

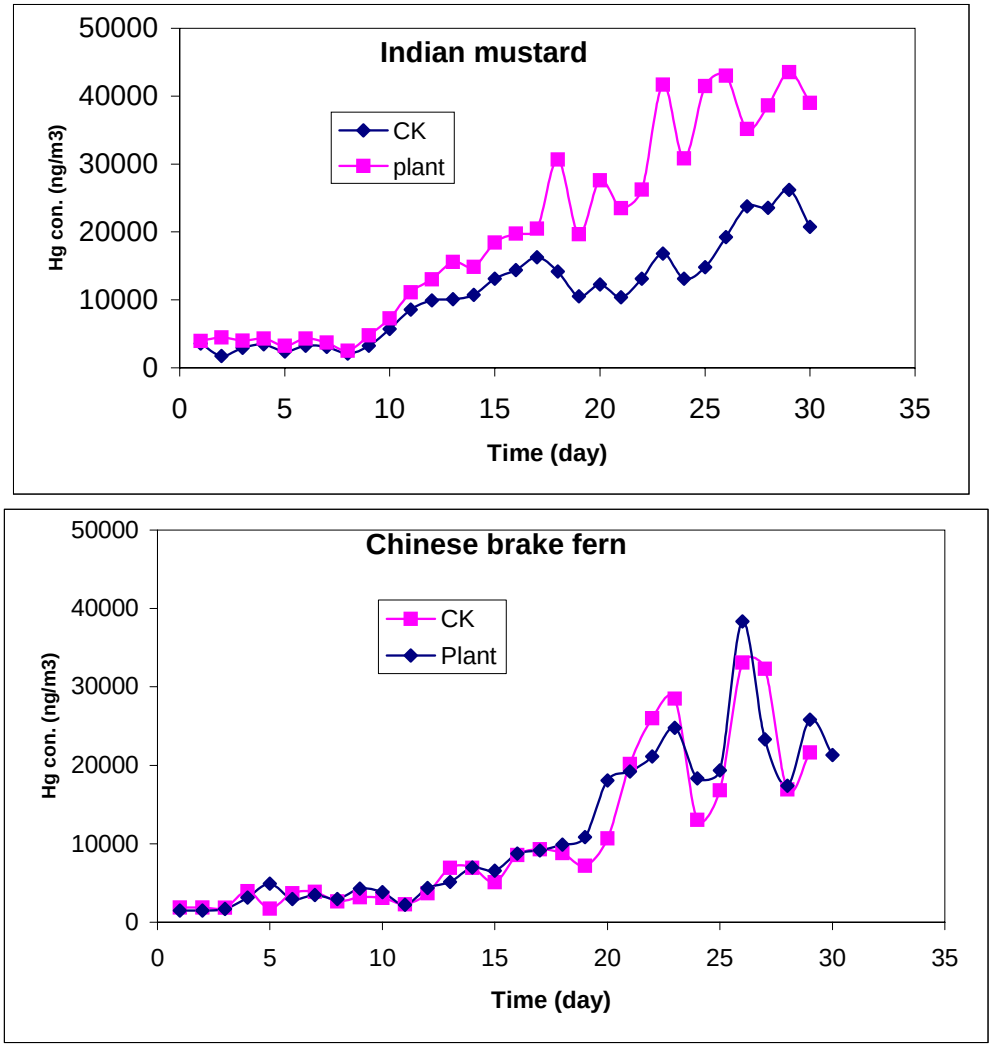

Figure 23. Hg concentrations in airs of two chambers equilibrated with 1 kg of Oak Ridge soil contaminated with 200 mg/kg Hg as HgCl2.

WORK FORECAST

Greenhouse studies on phytoremediation application of potential plants will continue.

Task 6

Saltstone

Ronald Palmer

INTRODUCTION

This project is comprised of two subtasks. The first consists of laboratory scale experiments designed to examine the thermal properties of new Saltstone formulations. The second consists of Pilot Scale studies.

Laboratory Scale Experiments

Small batches prepared in the laboratory must be done prior to designing the pilot scale tests. Lab methods will be set up for measuring the heat of hydration for various Saltstone formulations.

Mixers capable of providing batches from as small as several 10s of grams to more than one kilogram are available in the ICET laboratory. A standard protocol for making these small batches will be developed.

An adiabatic calorimeter will designed and built to measure the heat of hydration of the Saltstone formulations. This device will provide basic thermal property measurements. These data are important contributions to new revisions of the Performance Assessment documentation.

Pilot Scale Studies

Small batches prepared in the laboratory can only provide preliminary information. A pilot-scale facility, capable of producing 55-gallon drum sized product, is available at the ICET laboratories. Drums can be appropriately instrumented to examine the heat generation of Saltstone formulations on an intermediate scale between the laboratory and actual Saltstone production facility.

Using these same waste simulant recipes, various formulations of Saltstone will be produced at our pilot-scale facility. The laboratory scale work provides the basis for determining which formulations to study further. The results of this work will provide the confidence necessary for full scale production at the Saltstone production facility.

WORK ACCOMPLISMENT

Representatives of Savannah River visited ICET for a day of extended discussions and a tour of our facilities. The discussions included these topics:

Raw Materials Issues

There are several different sources and several different types of Portland cement, fly ash and slag. Careful consideration of materials utilization is required, especially as we strive to duplicate the SRS process as closely as possible. John Harbour, who has been studying this process at SRNL, has archived samples of the raw materials used in studies at SRNL for future reference.

Moisture content may also vary in the fly ash and slag, so the "age" of the materials is important. We may want to find a way to "standardize" the moisture content, perhaps using measurement by TGA as a guideline. (An inventory of the materials on hand at ICET will be taken and an assessment of their status made to determine their acceptability. These materials will be used for functional checkout of methods only. SRNL will provide the raw materials for the actual testing to provide better comparison with the work done at SRNL.)

The reagents for making up the salt solutions can be expensive, especially in large quantity for the pilot scale tests. Recommend just using tap water for the initial scoping tests and to confirm the operations. SRS will provide simulant batch sheets for the large-scale tests.

Adiabatic Calorimeter

The design, construction, and assembly of the ICET adiabatic calorimeter is going well. Good advice was received from the SRNL personnel who have done this before. Final assembly and some initial testing will be completed by the end of December.

The nominal tests will run for about one or two days. By that time, most of the reactions of interest should be complete. Building additional adiabatic calorimeter units were discussed, specifically concerning runs that would take a couple of weeks to run. For the present time, the need for additional adiabatic calorimeters is not required. This may change in the future.

SRNL will provide both raw materials and salt solutions so that isothermal calorimeter data obtained at SRNL can be compared to the adiabatic measurements at ICET.

Pilot Scale Testing

The SRNL representatives were pleased with the ICET method of making grout feed. The mixing system is more than adequate in mixing the dry material with the solution. We will assemble a thermocouple tree based on their design, with slight modifications to the structural support, and will be prepared to run an initial test using tap water in early 2009.

Specific Heat Measurements

John Harbour has been making some specific heat measurements using an isothermal calorimeter. SRNL representatives believe that the data from the initial work done by Steimke may be incorrect. We will investigate the possibility of using our Differential Scanning Calorimeter for making similar measurements.

Modeling

SRNL provided a paper by Si Young Lee on the heat transfer modeling of a 55-gallon drum using CFD, to determine the temperature distribution within and skin temperature. These data were compared to actual 55-gallon drum data, using data obtained from the isothermal calorimeter. SRNL will also provide ICET with a one-dimensional code presently used to determine the temperature distribution in the Saltstone vaults, based on Steimke's data. We will investigate creating a two-dimensional model to complement this one-dimensional code.

Work in the laboratory during this reporting period included:

- Establishing a protocol for making salt solutions and small batches of Saltstone formulations
- Designing and building an adiabatic calorimeter
- Designing experiments with 1kg batches studying the heat evolution of the Saltstone formulations using containers outfitted with thermocouples

WORK FORECAST

The following tasks are expected to be active during the next quarter:

- Continue to experiment with the protocol for making salt solutions and small batches of Saltstone formulations, including using water in place of the salt solution
- Complete the construction of an adiabatic calorimeter and run initial experiments using water
- Obtain the SRNL design for a thermocouple tree for measuring thermal behavior in pilot scale system and work toward its assembly and prepare for an initial pilot scale test in early 2009
- Investigate the possibility of adding a modeling task to this activity

REFERENCES

1. Steimke, J. L. and M. D. Fowley, "Measurement of Thermal Properties of Saltstone," WSRC TR-97-00357, Westinghouse Savannah River Company, Aiken, SC, 1997.

2. Harbour, J. R. et al., “Characterization of Slag, Fly Ash and Portland Cement for Saltstone,” WSRC-TR-2006-00067, Revision 0, Savannah River National Laboratory, Aiken, SC, 2006.
3. Harbour, J. R. et al., “Heat of Hydration of Saltstone Mixes – Measurement by Isothermal Calorimetry,” WSRC-STI-2007-00263, Revision 0, Savannah River National Laboratory, Aiken, SC, 2007.
4. Lee, Si Young, “Thermal Performance Analysis for WSB Drum,” WSRC-STI-2008-00262, Savannah River National Laboratory, Aiken, SC, May 2008.
5. Cozzi, A. D., et al., “Effect of Heat of Hydration on Drum Temperature and Filter Performance in Full-Scale Waste Solidification Building Simulated High Activity Waste Drums,” WSRC-STI-2008-00367, Revision 0, Savannah River National Laboratory, Aiken, SC, September 2008.

Task 7

Bioavailability Studies of Mercury and other Heavy Metal Contaminants in Ecosystems of Selected DOE Sights

Fengxiang X. Han, Yi Su, David L. Monts, and Charles A. Waggoner

INTRODUCTION

The majority of Hg in the floodplain soils of East Fork Poplar Creek, Oak Ridge, TN has been reported to be HgS. Most recently, the Hg levels in both water and fish were found to have increased. Thus, effects of Fe/Mn minerals on bioavailability and stability of HgS is important for better understanding the mechanisms responsible for the increase.

WORK ACCOMPLISHMENT

Details of oxidation kinetics of both pure HgS and Oak Ridge contaminated soils with Fe_2O_3 and Fe_3O_4 were re-investigated (Fig. 15). The results clearly indicate that the oxidation reactions were initially fast, followed by a plateau (Fig. 15). The sulfate produced was used to represent the oxidation rate. The S species in the reaction system was also identified (SO_4^{-2} and other intermediate S species). Magnetite had a higher potential in releasing of SO_4^{-2} from HgS contaminated Oak Ridge soils than hematite (Fig. 15).

The effects of Cl^- concentrations on oxidation of HgS from both pure and Oak Ridge contaminated soils indicate that Cl^- is a significant environmental factor controlling the potential release of Hg from contaminated soils (Figs. 16-18). The increase in Cl^- concentrations in soils and subsurface resulted in increasing the release of SO_4^{-2}, iron, and mercury as accompanied by the significant decrease in pH in both pure HgS system (Fig. 16-17) and HgS contaminated Oak Ridge soils when they were reacted with Fe oxides, especially magnetite (Fig. 18).

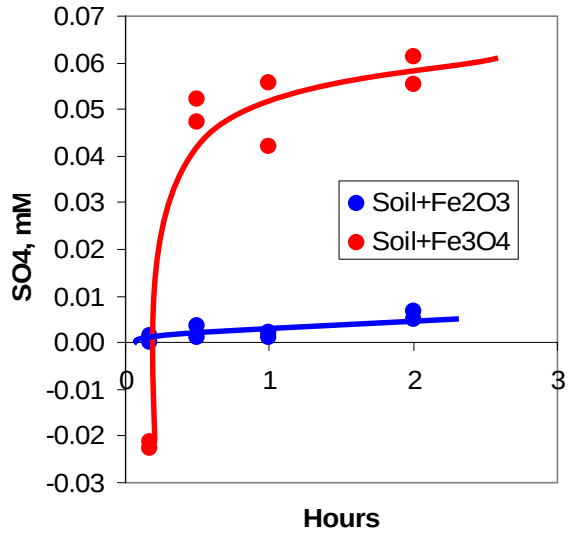

Figure 24. Sulfate release from Hg contaminated Oak Ridge soil (with 2000 mg/kg Hg as HgS) (5 g soil, 25 ml 0.01M $NaNO_3$ for 0.17 (10 min), 0.5, 1, 2 hrs).

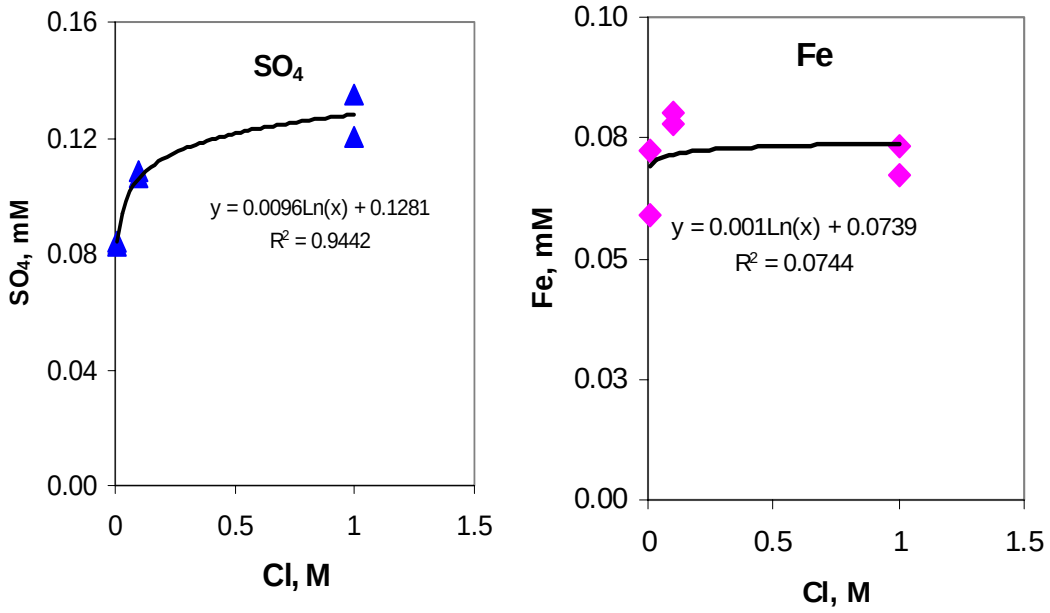

Figure 25. Effects of Cl^- concentrations (0.01, 0.1, 1 M Cl^-) on sulfate and iron release from pure HgS system reacted with HgS+Fe_3O_4 (Magnetite) (1 g Fe oxides, 0.1 g HgS, 35 ml 0.01M $NaNO_3$ for 24 hrs).

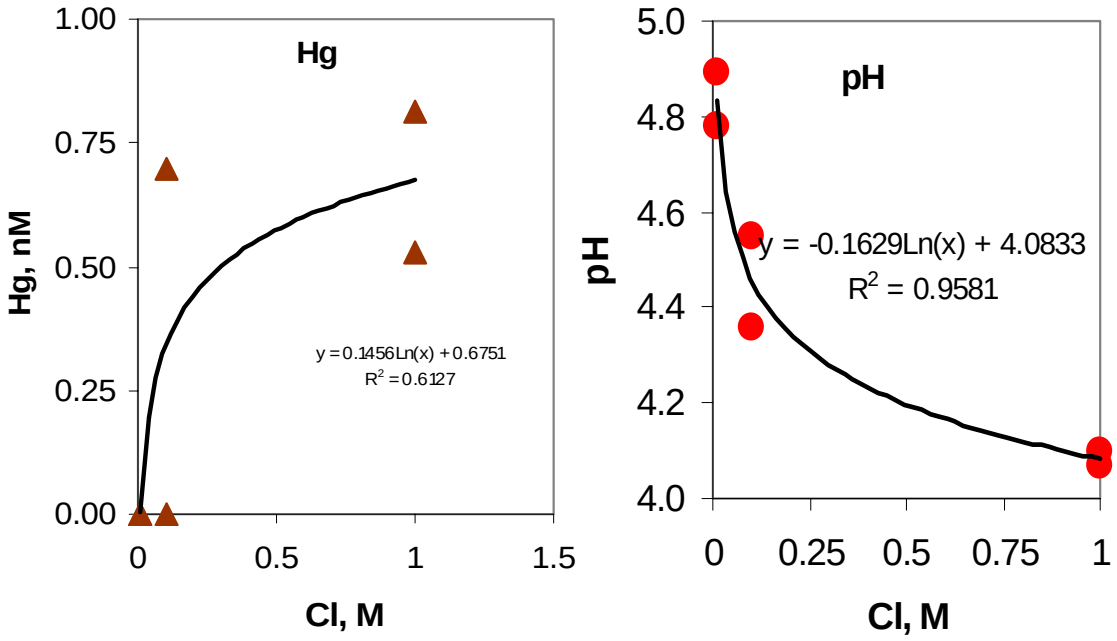

Figure 26. Effects of Cl^- concentrations (0.01, 0.1, 1 M Cl^-) on mercury and pH from pure HgS system reacted with HgS+Fe_3O_4 (Magnetite) (1 g Fe oxides, 0.1 g HgS, 35 ml 0.01M $NaNO_3$ for 24 hrs).

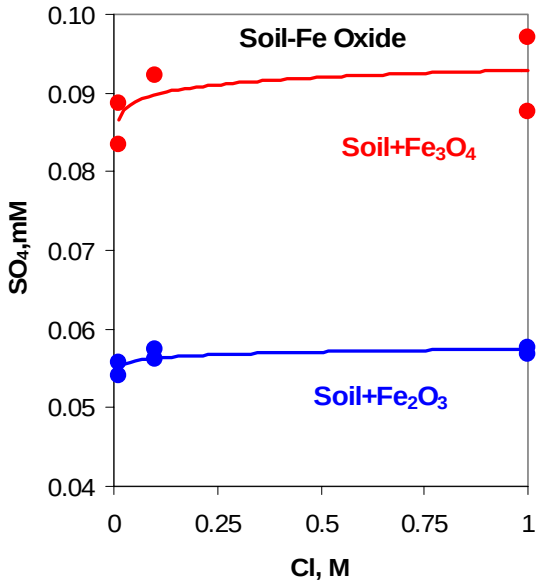

Figure 27. Effect of Cl^- concentrations on SO_4^{-2} release from Oak Ridge soil contaminated with 2000 mg/kg Hg as HgS (5 g soil, 35 ml 0.01M $NaNO_3$ for 24 hrs).

CONCLUSIONS

The results show that oxidation rate of HgS from HgS contaminated Oak Ridge soil was initially fast and increased until 30 min, then followed by the plateau. The 80-90% of S in the reaction system was SO_4^{-2} with a small amount of other intermediate S species. Cl^- significantly increased SO_4^{-2}, Fe, Hg concentrations in solution and decreased pH in both pure HgS system and contaminated Oak Ridge soil reacted with iron oxides.

WORK FORECAST

The effects of pH on release of oxidation of HgS as indicated by the release of SO_4^{-2} from both pure HgS and contaminated soils will be studied.

IN-TANK CHARACTERIZATION FOR CLOSURE OF HANFORD WASTE TANKS

David L. Monts

At end of the previous quarter, ICET was informed that because of the downward revision of the ICET Cooperative Agreement CA08 budget, that there are no funds to support the Hanford in-tank characterization effort for the current Cooperative Agreement year. ICET administrators subsequently issued a stop-work order. The bi-weekly conference calls with our Hanford collaborators were suspended. At this time, no further efforts are planned until funding becomes available.